Argonne NATIONAL LABORATORY

ANL/SSS-21/16

Modeling ^{233}Pa Generation in Thorium-fueled Reactors for Safeguards

Strategic Security Sciences Division

About Argonne National Laboratory

Argonne is a U.S. Department of Energy laboratory managed by UChicago Argonne, LLC under contract DE-AC02-06CH11357. The Laboratory's main facility is outside Chicago, at 9700 South Cass Avenue, Lemont, Illinois 60439. For information about Argonne and its pioneering science and technology programs, see www.anl.gov.

ANL/SSS-21/16

Modeling ^{233}Pa Generation in Thorium-fueled Reactors for Safeguards

prepared by
Victoria Davis
Strategic Security Sciences Division, Argonne National Laboratory
Department of Mechanical and Nuclear Engineering, Virginia Commonwealth University

Braden Goddard
Department of Mechanical and Nuclear Engineering, Virginia Commonwealth University

George W. Hitt
Department of Physics and Engineering Science, Coastal Carolina University

Scott Richards
Nuclear Science and Engineering Division, Argonne National Laboratory

Claudio Gariazzo
Strategic Security Sciences Division, Argonne National Laboratory

Prepared for the DOE/NNSA Office of International Nuclear Safeguards

December 2021

CONTENTS

FIGURES

EXECUTIVE SUMMARY

Thorium has been considered as a possible alternative to uranium for nuclear fuel for many decades. It is three to four times more abundant in the earth than uranium and produces significantly less long-lived transuranic nuclear waste. There are those who think that thorium poses fewer proliferation concerns than other fuel types, largely due to ^{232}U buildup (and associated high-energy gamma-emitting decay products) in the irradiated thorium fuel. However, to fully explore potential international safeguards concerns, the production and subsequent decay of ^{233}Pa produced in the reactor core still must be studied. With its half-life of 27 days, ^{233}Pa decays to ^{233}U, which is an International Atomic Energy Agency (IAEA) defined special fissionable material that can be used for nuclear weapons production.

With more research being dedicated to thorium-fueled reactors, and since several of these reactor designs include online fuel processing (allowing for on-site protactinium separation), it is important to study potential proliferation concerns. It is theoretically possible to extract protactinium (Pa) from the irradiated fuel before the activated thorium decays into ^{233}U. This hypothetical pathway can become an even greater proliferation concern if the extracted protactinium is purified through a second separation of protactinium isotopes approximately ten days later to remove the short half-life decay products of ^{232}Pa and ^{234}Pa, thus resulting in a higher concentration of the ^{233}Pa isotope—a direct parent radionuclide of weapons-usable ^{233}U.

To mitigate this safeguards challenge associated with this potential pathway, different nuclear material accountancy (NMA) techniques were reviewed for their ability to quantify ^{233}Pa extracted from irradiated thorium fuel. Quantifying and tracking ^{233}Pa is important for safeguards because ^{233}Pa is a precursor for ^{233}U—special fissionable material that should be under IAEA safeguards. If ^{233}Pa is not monitored, it is possible to produce high purity ^{233}U outside of the safeguards monitoring system. The most important characteristics of different NMA techniques were technology maturity, cost, precision, and time to acquire results. Some technologies, like hybrid K-edge densitometry (HKED) and passive gamma spectroscopy, appear to be viable techniques based on current literature. However, due to the limited scope of this project, only passive gamma spectroscopy was further investigated.

Three different reactor types—pressurized water reactor (PWR), Canada deuterium uranium (CANDU) reactor, and molten salt reactor (MSR)—were modeled with mixed thorium-uranium oxide fuels that were burned until the fuel was spent. The protactinium in the used fuel was extracted at the time of shutdown and the change in isotopic content of the protactinium quantified. Gamma spectroscopy simulations were performed for the protactinium isotopes and their decay products at various decay times to understand protactinium generation within the reactor cores. Given the simplicity of the models and the large assumptions made (e.g., no background, no shielding, no self-attenuation), the initial results indicate that though ^{233}Pa is detectable for each reactor fuel type modeled at all decay times (0 to 300 days), more work should be completed with higher fidelity models.

Acknowledgements

This work was funded by the Department of Energy's National Nuclear Security Administration Office of International Nuclear Safeguards (NA-241).

INTRODUCTION

Thorium has been considered a possible alternative to uranium for nuclear fuel for many decades. It is three to four times more abundant in the earth than uranium and produces significantly less long-lived transuranic nuclear waste. Some claim that thorium poses fewer proliferation concerns than other fuel types, largely due to ^{232}U buildup (and associated high energy gamma-emitting decay products) in the irradiated thorium fuel, but this is not a factor for international safeguards [1]. To fully explore potential proliferation concerns and safeguards challenges posed by thorium fuel cycles, production and subsequent decay of ^{233}Pa produced in these thorium-fueled reactor cores must be studied. With a half-life of 27 days, ^{233}Pa decays to ^{233}U, which is an International Atomic Energy Agency (IAEA) defined special fissionable material that can be used for nuclear weapons production [2]. With more research being dedicated to thorium-fueled reactors, and with several of these reactor designs possessing online fuel processing (allowing for on-site protactinium separation), it is important to understand potential proliferation pathways that pose a challenge to international safeguards. It is theoretically possible to extract ^{233}Pa from the irradiated fuel salt before it decays into ^{233}U. This hypothetical potential diversion can become an even greater concern if the extracted protactinium is purified through a second separation of protactinium isotopes approximately ten days later to remove the short half-life decay products of ^{232}Pa and ^{234}Pa. This would result in a higher concentration of the ^{233}Pa isotope—a direct parent radionuclide of ^{233}U.

Many countries have shown interest in thorium-fueled nuclear reactors, and many different designs have been researched [3]: Canada and China have worked on Canada deuterium uranium (CANDU) reactors, India designed an advanced heavy water reactor, Germany, Brazil, Norway, and Russia have all researched pressurized light water reactors, Germany and the UK have operated high-temperature gas-cooled reactors, and research is ongoing for molten-salt reactors in China, Japan, Russia, France, and the United States. The potential widespread use of next-generation thorium-fueled reactors compels the international safeguards community to assess the ramifications of increased global ^{233}U production through its ^{233}Pa vector.

Background: Thorium-Fueled Reactors

There are many different types of nuclear reactors that can use thorium-based fuel. The most common is the pressurized water reactor (PWR), a type of light water reactor. Its schematic is shown in Figure 1. Generally, these reactors use enriched uranium (3%–5% ^{235}U) oxide fuel contained in fuel rods. PWRs usually have about 150–250 fuel assemblies, each containing about 200–300 fuel rods. The moderator and coolant are both light water.

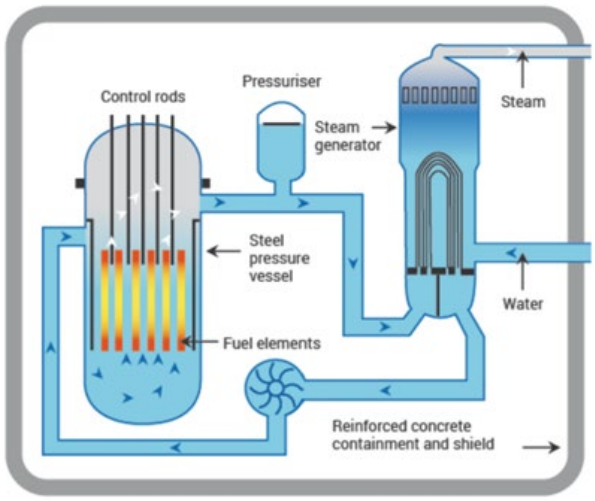

Figure 1: Diagram of a pressurized water reactor (PWR) [4].

Another type of reactor is the pressurized heavy water reactor (PHWR), the most common type being a CANDU reactor (schematic shown in Figure 2). No PHWRs are in commercial use in the United States, but they can be seen in many countries throughout the world. They function much like PWRs, but they use deuterium oxide (heavy water) as the moderator, and some variations use light water as the coolant. PHWRs generally use natural uranium (0.711% ^{235}U) for the fuel, although a wide spectrum of different fuel enrichments and compositions have been tested in PHWRs.

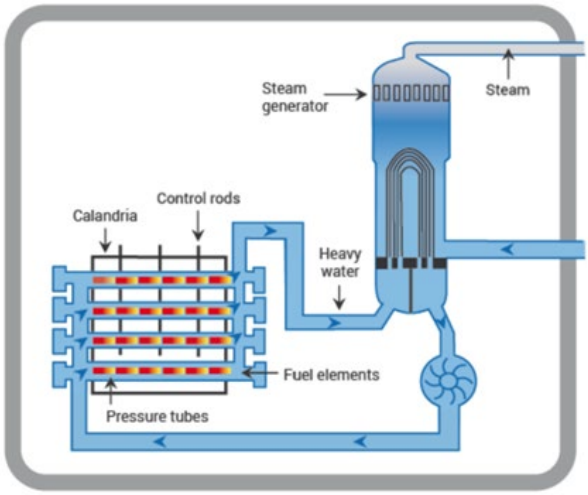

Figure 2: Diagram of a pressurized heavy water reactor (PHWR)[4].

Molten salt reactors (MSRs), are another type of reactor that is being heavily researched for possible use with uranium or thorium fuels (schematic shown in Figure 3) [3]. Unlike current generation nuclear reactors, MSRs use molten salt as the coolant rather than water. Most MSR concepts also use liquid fuel rather than solid fuel [5]. The fuel is combined with a liquid salt mixture, usually lithium-beryllium fluoride. The fuel itself could be thorium, uranium, or plutonium fluoride. In some designs, graphite is used as a moderator. MSRs can have single-fluid or two-fluid designs. Two-fluid MSRs improve the breeding capabilities of the reactor: The reactor has one fluid as a breeder fluid and one fluid as fuel. The breeder

would include thorium fluoride, which would produce ^{233}U, which could then be used in the fuel fluid as fissile material. A single-fluid design would simply have one fluid containing the fuel and coolant [6]. As shown in Figure 3, many MSR designs include online reprocessing of the fuel salt, so that some of the irradiated fuel may be removed for a time from the reactor core for treatment and combined with fresh fuel salt before being returned to the core. The concept of the MSR has been around for many decades; however, they are not yet widely used. With more research being invested in MSRs, some anticipate their use in the near future.

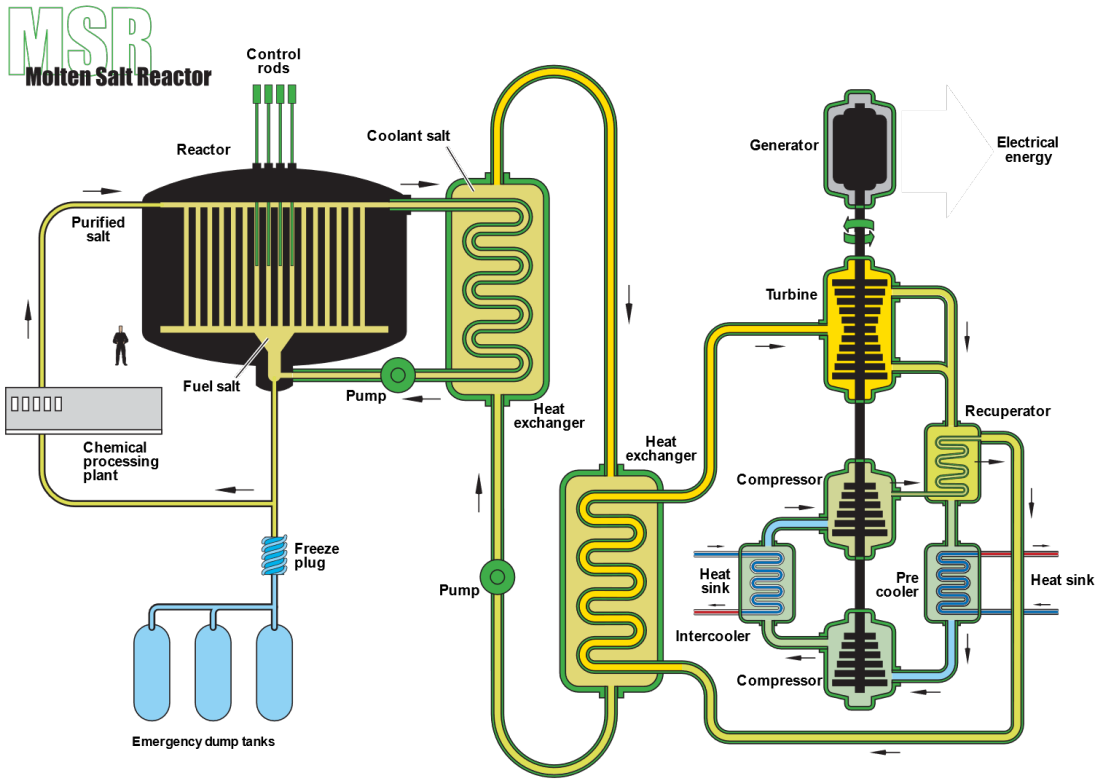

Figure 3: Diagram of a molten salt reactor (MSR) [7].

MSRs present new challenges that are not seen in other reactor designs [5]. Many have fuel, coolant, fission products, and actinides mixed in one homogeneous liquid. MSR fuel is not contained in fuel assemblies, and, as noted above, many designs employ an online reprocessing capability in which irradiated fuel salt that has been removed from the reactor core is treated before being returned to the reactor core while the reactor is in operation. Current material accountancy methods are ill-equipped for dealing with the new challenges of the MSR. Since the fuel is liquid, the isotopic concentration will be continuously varying. It would also be quite difficult to take passive radiation-based measurements, because the fuel is highly radioactive and the reactor operates at very high temperatures. Furthermore, with liquid fissile material, challenges arise in defining the appropriate nuclear material accountancy (NMA) approaches to item versus bulk accounting facilities or defining strategic measurement points. On this topic, the IAEA states:

> "Designers should be aware that such reactors cannot be considered item facilities… [and] more stringent nuclear material accountancy measures will likely be required to verify the quantities, locations and movements of the nuclear material. These measures can include, but are not limited to, fuel flow monitors, seals, video surveillance, the use of sensors to trigger other sensors, more

> accurate NDA measurements and sampling plans... Most of this instrumentation does not yet exist and a significant R&D effort can be expected" [8].

Clearly, current NMA methods are not satisfactory for MSRs: Using thorium fuel adds complexity to the already challenging quantification of nuclear material in an operational MSR. Because of the numerous complications in defining appropriate safeguards approaches for MSRs, many have proposed developing innovative safeguards measures in conjunction with facility designers (i.e., safeguards-by-design or SBD) in the initial stages of MSR development [9]. The IAEA defines SBD as "the process of including international safeguards considerations throughout all phases of a nuclear facility life cycle; from the initial conceptual design to facility construction and into operations, including design modifications and decommissioning. Good systems engineering practice requires the inclusion of all relevant requirements early in the design process to optimize the system to perform effectively at the lowest cost and minimum risk" [8]. Developing safeguard measures via SBD would advance the IAEA's and the international nuclear safeguards community's understanding of implementing proper safeguards techniques for MSRs.

POTENTIAL THORIUM-FUELED REACTOR SAFEGUARDS CHALLENGES

The majority of thorium-based fuel consists of the ^{232}Th isotope. In the reactor, ^{232}Th absorbs a neutron and becomes ^{233}Th. Subsequently, ^{233}Th beta decays (with a half-life of 22 minutes) to ^{233}Pa, which in turn beta decays with a half-life of 27 days to ^{233}U [1,10]. The full reaction and decay paths of ^{232}Th are shown in Figure 4. ^{233}U falls under international safeguards as it is classified as direct use material [1] —but ^{233}Pa does not. As such, measures implemented by the State and the IAEA do not measure or account for ^{233}Pa, which could potentially lead to a proliferation concern like unmonitored production and diversion of ^{233}U.

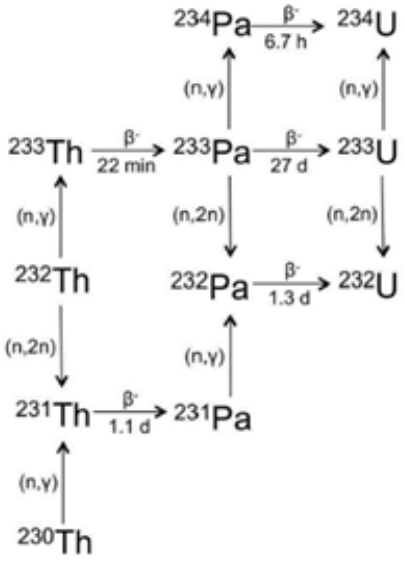

Figure 4: ^{232}Th absorbs a neutron to become ^{233}Th and then beta decays twice to become ^{233}U [10].

The IAEA defines ^{233}U as special fissionable material [11]. Specifically, the IAEA Statute in Article XXI states "the term 'special fissionable material' means plutonium-239; uranium-233; uranium enriched in the isotopes 235 or 233; any material containing one or more of the foregoing; and such other fissionable material as the Board of Governors shall from time to time determine; but the term 'special fissionable material' does not include source material" [11]. The IAEA specifies in the *IAEA Safeguards Glossary* that any quantity of ^{233}U over 8 kg is considered a "significant quantity," which is "the approximate amount of nuclear material for which the possibility of manufacturing a nuclear explosive device cannot be excluded" [2]. In the same document, the IAEA also defines "safeguards" as "the timely detection of diversion of significant quantities of nuclear material from peaceful nuclear activities to the manufacture of nuclear weapons or of other nuclear explosive devices or for purposes unknown, and deterrence of such diversion by the risk of early detection" [2].

Despite its lack of official designation, if left to decay, diverted ^{233}Pa can produce quantities of ^{233}U which could fall outside of safeguards. If enough ^{233}Pa is diverted, the significant quantity of 8 kg of ^{233}U could eventually be reached. Given the decay relationship between ^{233}Pa and ^{233}U, it may be advisable for the IAEA to include it in the list of materials monitored by the IAEA. The issue of the authority to monitor ^{233}Pa is important and must be explored further, but it is beyond the scope of this project.

It is useful to examine the products of the thorium nuclear fuel cycle to determine if ^{233}Pa could be easily removed from the reactor without detection. This particularly becomes an issue for certain MSR concepts under development. In several MSR designs, fuel salt is removed from the reactor core and protactinium is deliberately separated [12]. Removing protactinium from the core reduces the potential for neutron

reactions that will transmute ^{233}Pa to other isotopes of protactinium. As shown in Figure 4, ^{233}Pa can absorb a low-energy ("thermal") neutron to become ^{234}Pa, which quickly beta decays to become non-fissile ^{234}U, and it can undergo a (n,2n) reaction with a high-energy ("fast") neutron to become ^{232}Pa, which beta decays to become ^{232}U. Away from the presence of bombarding neutrons, ^{233}Pa beta decays to ^{233}U [10]. The ^{233}U can then be added back into the reactor core as fissile fuel [13].

When protactinium is separated from the fuel salt, it inevitably includes some ^{232}Pa and ^{234}Pa. After 10 days there would be a large decrease of ^{232}Pa and ^{234}Pa present due to their short half-lives, leaving ^{233}Pa to make up a larger fraction of the protactinium isotopes in the mixture. At this time, a second separation of protactinium from the uranium and other decay products can be performed, and the separated protactinium can be left to decay again, where its high ^{233}Pa content eventually yields a higher purity of ^{233}U. Figure 5 shows that, even after 10 days (240 hours), there are minuscule amounts of ^{232}Pa and ^{234}Pa left. This could increase the proliferation concern regarding reactors where fuel can be reprocessed shortly after leaving the reactor. The presence of ^{232}U may offer some defense against diversion and weaponization due to decay products (such as ^{208}Tl) that emit high energy gamma rays [13], which would require more safety measures for handling the material, make it more detectable, and add other challenges for potential diversion and material accountancy for safeguards verification purposes [14,15].

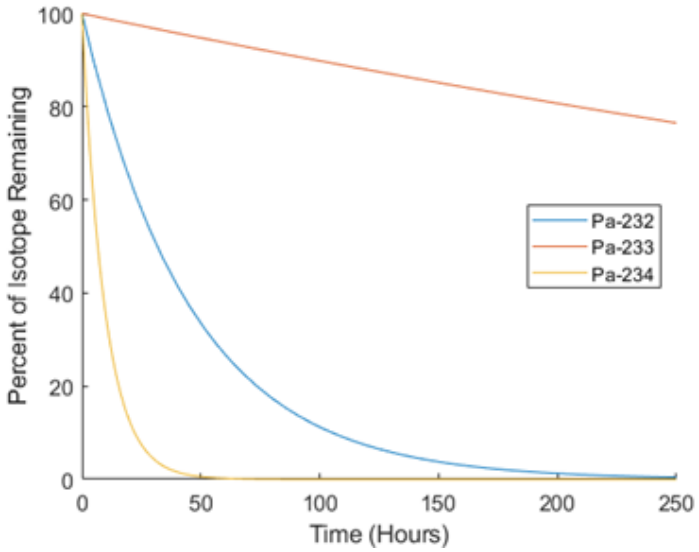

Figure 5: Decay of ^{232}Pa, ^{233}Pa, and ^{234}Pa after being separated from the thorium fuel.

EVALUATION OF NUCLEAR MATERIAL ACCOUNTANCY TECHNIQUES

Under IAEA safeguards, many NMA techniques, including both destructive assay (DA) and non-destructive assay (NDA) technologies, are used to account for nuclear materials in facilities. In the following section, material measurement techniques for the detection of ^{233}Pa were identified and their assay capabilities evaluated to identify a viable and practical technique. Many factors fed into this evaluation, including technology maturity, cost, precision, and duration to acquire results.

Destructive Assay Techniques

According to the *IAEA Safeguards Glossary*, destructive assay (DA) is the "determination of nuclear material content and, if required, of the isotopic composition of chemical elements present in the sample. Destructive analysis normally involves destruction of the physical form of the sample" [2]. In both techniques below, spent fuel content would have to be extracted and converted into a solution for analysis. Though not a technical challenge, fuel dissolution would require additional preparatory steps prior to analysis.

Mass Spectrometry

Mass spectrometry identifies elements by converting molecules to ions and then measuring the mass-to-charge ratio of the ions [16,17,18,19,20]. Traditional mass spectrometry techniques require relatively large sample sizes and can take days or weeks to obtain results, which is less than ideal for facilities with short material balance periods [21]. This includes techniques such as thermal ionization mass spectrometry (TIMS) and inductively coupled plasma mass spectrometry (ICP-MS). However, a technique called laser ablation multi-collector inductively coupled plasma mass spectrometry (LA-MC-ICP-MS) offers the advantage of requiring smaller sample sizes and has been shown to be a rapid mass spectrometry technique that does not require the same chemical preparation as other techniques [22]. In this technique, the laser is used to ablate a small sample that can then be used in the ICP-MS.

Mass spectrometry is generally considered to be a mature technique that has high capital and operational costs. It is considered the gold standard for measurement precision, but results take a considerable amount of time to acquire. With the relatively short half-lives of the protactinium isotopes, this technique may not be applicable due to radioactive decay during sample preparation.

Gravimetry

Gravimetry measures the weight of a substance, which in turn can be correlated to mass. There are four main types of gravimetry: precipitation gravimetry, volatilization gravimetry, particulate gravimetry, and electrogravimetry [23].

- Precipitation gravimetry relies on the addition of a precipitant to a solution containing the analyte. Once the precipitate and analyte react and precipitation occurs, the precipitate is separated from the solution and analyzed. For large samples, a relative error of 0.1%–0.2% is generally reached with a precision of several parts per million. This technique is well-known and inexpensive; however, it is time intensive. With newer techniques available, precipitation gravimetry is becoming less commonly used.
- Volatilization gravimetry involves thermally or chemically decomposing the sample and measuring the change in mass during this process. Volatilization gravimetry's accuracy and precision is similar to precipitation gravimetry's, but it is also a time-intensive technique.
- Particulate gravimetry separates an analyte that is already in a form that is easy to remove from the mixture without needing a chemical reaction. This separation can be done through filtration or

extraction. This technique generally has the same accuracy and precision as precipitation and volatilization gravimetry.

- Electrogravimetry uses an electrode and the application of a current or potential [24] to "plate" the electrode with the analyte. The electrode is weighed before and after the current or potential is applied. The concentration of the analyte can be determined through this change in mass of the electrode.

In general, gravimetry techniques are quite mature and precise, but they take a relatively long time to obtain results. With the relatively short half-lives of the protactinium isotopes, gravimetry is not a preferred technique, as the ratios of the isotopes may significantly change during the measurement.

Non-Destructive Assay Techniques

According to the *IAEA Safeguards Glossary*, non-destructive assay (NDA) is "a measurement of the nuclear material content or of the element or isotopic concentration of an item without producing significant physical or chemical changes in the item. It is generally carried out by observing the radiometric emission or response from the item and by comparing that emission or response with a calibration based on essentially similar items whose contents have been determined through destructive analysis" [2]. NDA techniques may rely on either passive or induced (i.e., active) measurements for readings, and they require minimal preliminary sample preparation, unlike DA techniques.

Passive Total Neutron Counting

Passive total neutron counting counts all passively emitted neutrons from a sample regardless of their source, time correlation, or initial energy [25]. These neutrons can come from alpha-neutron (α, n) reactions or spontaneous fissions, often with small contributions from other background sources. Since ^{233}Pa does not emit neutrons (either via spontaneous fission or alpha-neutron reactions), passive total neutron counting is not a suitable technique for measuring ^{233}Pa.

Passive Neutron Coincidence Counting

Radionuclides that spontaneously fission create neutrons in multiples (doubles and triples) with neutron multiplet signatures that can be isolated from other neutron sources, such as alpha-neutron (α, n) reactions [21]. This technique works well for radionuclides with a relatively high probability of spontaneous fission, such as some plutonium isotopes, californium, and curium. However, as previously mentioned, ^{233}Pa does not spontaneously fission nor does any of its decay products. Therefore, this technique will not work for the measurement of ^{233}Pa.

Active Neutron Interrogation

For some materials that do not spontaneously fission nor produce neutrons, it is possible to interrogate the sample with an external neutron source to induce fission. There are several neutron interrogation techniques. One technique is to use active well coincidence counters (AWCCs), which consist of a sample cavity surrounded by ^{3}He tubes embedded in polyethylene blocks, with an (α, n) neutron source located at one end (or both ends) of the cylindrical sample cavity [26]. Another active neutron interrogation technique uses a californium source to induce fission in a sample for a very short amount of time. After removing the source, delayed neutrons are counted and correlated to effective fissile mass. All active neutron interrogation techniques are unlikely to provide useful information when measuring ^{233}Pa samples due to the nuclide's relatively small fission cross section (even at neutron energies above 1 MeV). This can be seen in Figure 6, which displays the neutron-induced fission cross section for ^{233}Pa along with that of ^{235}U for comparison.

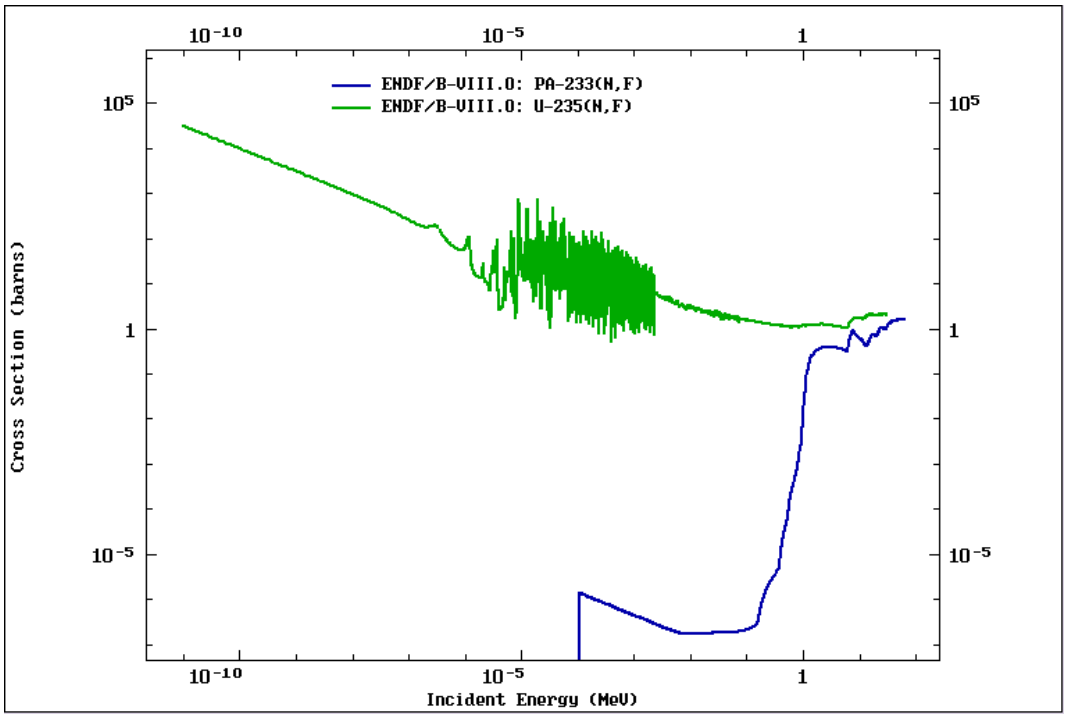

Figure 6: Induced fission cross section for ^{233}Pa (lower red curve) and ^{235}U (upper blue curve) [27].

Hybrid K-Edge Densitometry

Hybrid k-edge densitometry (HKED) combines x-ray fluorescence (XRF) and k-edge densitometry (KED). KED works by passing x-rays above and below the k-absorption energies for elements of interest in the measurement sample [21,28]. The size of the discontinuity at the k-absorption edge can be correlated to the concentration of the element. XRF can be used to measure the intensity of induced x-rays in the measurement sample, thus quantifying the total mass of the element of interest in the sample. The combination of these two techniques lowers the measurement uncertainty and allows for the absolute concentration of each element to be determined. This technique is promising since it can be used onsite and could allow for close to real-time measurements. Precision of ~0.5% can be achieved with measurement durations of 5-20 minutes [29]. HKED is a mature technology with commercial systems available; however, the costs of these systems are moderate to high and require a moderate amount of floor space.

Laser-Induced Breakdown Spectroscopy

Laser-induced breakdown spectroscopy (LIBS) works by hitting a small portion of the sample material with a laser, producing a high-energy plasma [30]. As the plasma cools, atoms relax from excited states back to ground states and emit light. LIBS spectral analysis can determine the elements emitting each spectral peak. This technique is not mature yet and needs more research and development before it can be conclusively evaluated as a possible technique for ^{233}Pa assay. It also can be noted that LIBS is not entirely an NDA technique, since a small portion of the material is destroyed during the measurement process.

Calorimetry

Calorimetry is a technique of measuring heat produced by different materials during chemical processes to determine the mass of each [31,32,33]. This technique has been used for around 45 years and has become a primary technique in the United States for the assay of plutonium and tritium for nuclear material accountability [34]. While this technique is commonly used and quite accurate, it takes a relatively long

time to acquire results compared to other NDA techniques. As previously mentioned, ^{233}Pa has a half-life of 27 days, and the other protactinium isotopes have even shorter half-lives. With a time delay for results, the relative concentrations of the protactinium isotopes can change by a significant amount. Although calorimetry is a mature technique, a quicker technique is required, and so calorimetry is impractical for the purpose of measuring protactinium.

Passive Gamma Spectroscopy

Gamma spectroscopy measures gamma-ray emissions and their energy distribution from radionuclides when they undergo radioactive decay [35,36]. Each radionuclide has its own unique gamma spectrum that can aid in the identification of the nuclide. Some radionuclides have a clear gamma spectrum with high yield gamma lines that are well separated in energy, while others can have complicated gamma spectra that are difficult to use for identification, having only a few gamma lines with low yields that are spaced close in energy to each other or gammas from other radionuclides.

Gamma spectroscopy is a mature technique, can be fairly inexpensive when compared to other NDA measures, especially when a sodium iodide (NaI) detector is used, and produces results relatively quickly (within minutes). The precision of gamma spectroscopy varies with the detector material used and the nuclear material being measured. Often this technique is used to acquire isotopic ratios, which, when combined with other NDA techniques such as neutron multiplicity counting, can provide isotopic masses in a sample. In particular, ^{233}Pa exhibits several characteristic high-intensity gamma peaks, of which five can be used for signifying its presence (due to probabilities of emission with over 1% yield): 300 keV, 312 keV, 340 keV, 398 keV, and 416 keV. With these five peaks, the gamma spectrum of extracted ^{233}Pa can be easily identified, assuming minimal background radiation. There should be no need for longer measurement times due to low count rates since ^{233}Pa has a specific photon emission rate (gamma rays created per second per gram) of 1.0×10^{15}. This is almost eight orders of magnitude larger than that of ^{233}U at 2.5×10^{7}. For these reasons, in this research the gamma spectroscopy technique was the primary focus for measuring ^{233}Pa in the separated protactinium mixture from thorium-based fuels.

SIMULATIONS

To understand protactinium gamma spectra, radiation transport detector measurements were simulated using Monte Carlo N-Particle (MCNP) code version 6.2 [37]. Specifically, ^{232}Pa, ^{233}Pa, and ^{234}Pa, along with their decay products (^{208}Tl, ^{212}Bi, ^{212}Pb, ^{216}Po, ^{220}Rn, ^{224}Ra, ^{225}Ra, ^{226}Ra, ^{228}Ra, ^{228}Th, ^{229}Th, ^{230}Th, ^{232}Th, ^{232}U, ^{233}U, ^{234}U), were simulated separately. The software RadSrc was used to generate the discrete gamma line energies needed for the source definition in the MCNP simulations [38]. The configuration of each simulation consisted of a point source of the radionuclide and a detector with its front face located 10 cm away. Two different types of detectors were simulated: a 2" x 2" NaI crystal-based detector and a 2" x 2" high-purity germanium (HPGe) coaxial detector. The former type of detector has low energy resolution but is less expensive and can operate at room temperature. The latter detector has a higher energy resolution but requires very low operating temperatures (about 77 K) and exhibits sensitivity to neutron irradiation damage. In-field usage of HPGe detectors can create additional engineering challenges depending on the facility layout and operational plan. In addition to being noticeably less expensive, NaI detectors are generally easier to model than HPGe detectors, despite requiring frequent recalibration due to a tendency toward energy calibration drift with changing environmental conditions.

Simulating each radionuclide separately allowed the unique gamma spectrum to be clearly shown for each individual radionuclide. These spectra can then be compared to a more realistic mixed source to identify the radionuclides that are present in the source. The ^{233}Pa spectrum in Figure 7 shows that certain gamma energies have high intensities and aid in the identification of this radionuclide. The gamma spectra for ^{232}Pa and ^{234}Pa are included in Appendix A.

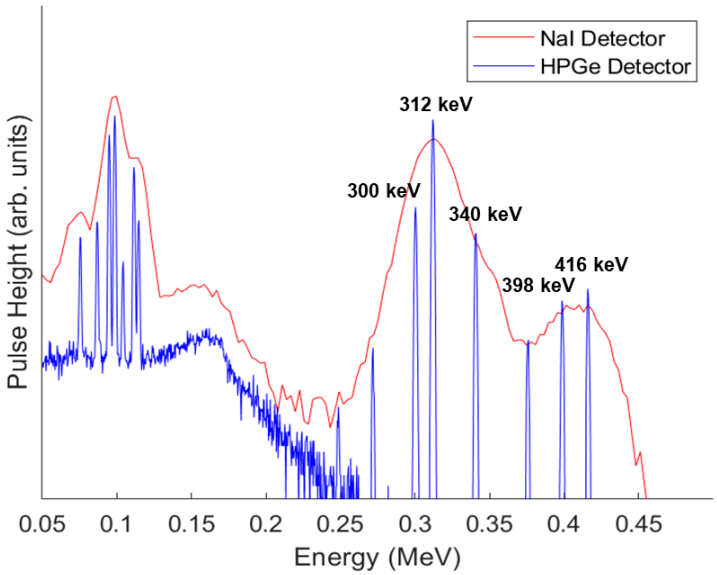

Figure 7: Gamma spectrum for ^{233}Pa showing high-intensity energies, most notably at 300 keV, 312 keV, 340 keV, 398 keV, and 416 keV. This gamma spectrum was produced using both a NaI detector (red) and a HPGe detector (blue) in MCNP.

To create a mixed source with the correct isotopic distribution of protactinium isotopes, nuclear reactor simulations were created using MCNP and ORIGEN2—a well-established reactor burnup (a measure of how much heavy metal has undergone nuclear fission) code that is relatively easy to use and provides computations in seconds. ORIGEN2 is also advantageous because it captures the full core, rather than just an individual fuel pin or assembly. The primary disadvantage of ORIGEN2 is that it has not been updated since June of 2002 and is only validated for certain fuel compositions [39]. Fuel compositions outside of

its validation range could create a neutron energy spectrum different from the model, thus leading to inaccurate used-fuel compositions. In contrast to ORIGEN2's zero-dimensional point models, MCNP allows for three-dimensional geometries. MCNP also does not make any assumptions about the neutron energy spectrum, but instead recalculates the spectrum for each time step based on the current fuel composition. This allows any fuel composition to be simulated and the simulations to be valid for a wider range of burnups. MCNP is frequently updated, with the newest version, 6.2, being released in 2018 [37]. The primary disadvantage of MCNP is that the input to the simulation can take more time to create, and the execution of the code takes longer, especially for burnup simulations. To decrease the length of these simulations and the complexity of the input, often only a single pin or a fuel assembly is modeled. Reflective boundary conditions can be included to create an infinite array of fuel pins, which is valid for pins in the center of the reactor but will produce incorrect results for pins on the outer edge of a reactor. For these reasons, both ORIGEN2 and MCNP 6.2 burnup simulations were performed.

ORIGEN2 Burnup

Four different reactor types were modeled in ORIGEN2 [40] to simulate burnup. Typical ranges of burnups for PWRs at the time they are shut down for refueling occur between 40 and 50 GWd/MTHM,[*] whereas for PHWRs, this number is much lower (typically 7.5 GWd/tHM for CANDU with natural uranium fuel) [41].

The first reactor modeled was a mixed thorium/uranium oxide-fueled PWR (called PWRUS in ORIGEN2) with an actinide mixture of 80% Th and 20% U with an enrichment of 19.9% ^{235}U and a burnup of 47 GWd/MTHM [42]. The second reactor was also a PWR (called PWRD5D35 in ORIGEN2) with the same inputs but a slightly different neutron energy flux profile. This fuel composition was chosen because it has approximately the same initial fissile atom density (^{235}U) as fuel with a 100% uranium actinide content but an enrichment of only 4% ^{235}U. In theory, higher uranium enrichments could be used to further reduce the mass of uranium while still maintaining the initial fissile atom density, but enrichments at or above 20% are considered highly enriched uranium (HEU) and create additional proliferation concerns. For the third reactor, a CANDU (called CANDUNAU in ORIGEN2) reactor was used with 19% Th and 81% U with an enrichment of 0.71%. This reactor had a burnup of 19 GWd/MTHM. This fuel composition represents the limit of how much thorium can be added to natural uranium while still maintaining criticality in a CANDU style reactor. Lastly, another CANDU (called CANDUSEU in ORIGEN2) reactor was modeled with 91% Th and 9% U with an enrichment of 20% and a burnup of 14 GWd/MTHM [43].

Each of the reactor simulations was set to return fuel composition values for continuous durations of 0, 0.1, 1, 3, 10, 30, 100, and 300 days after reactor shut down. For each of these time steps, a different protactinium composition was observed. This represents what the protactinium composition would look like if reprocessing took place at different decay times. While it is unrealistic to think that PWR or CANDU fuel can be reprocessed immediately after discharge, a simulation of this type does provide data points allowing for interpretation and extrapolation for extreme situations. These extracted protactinium quantities were all plotted for each reactor type over time, from immediate discharge to 300 days. The graphed ORIGEN2 output for the PWRUS is shown in Figure 8. The output for the other reactors can be seen in Appendix B.

[*] Burnup is commonly specified in megawatt-days or gigawatt-days of thermal output per metric ton of heavy metal (MWDT/MTHM or GWDT/MTHM).

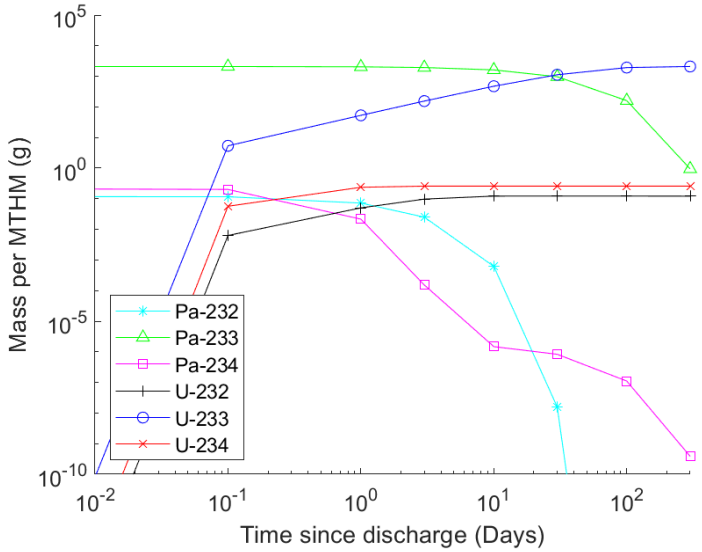

Figure 8: Relative abundance of the separated protactinium isotopes and the uranium produced from decay present in the separated fuel, from soon after discharge to 300 days post-discharge for the PWRUS.

The MCNP radiation detector simulation spectra and the ORIGEN2 simulation of protactinium mass quantities in the used fuel were then combined to create the mixed gamma spectrum of only ^{232}Pa, ^{233}Pa, and ^{234}Pa and their decay products, representing what a gamma spectrum of extracted protactinium from the used fuel would look like. Gamma spectra were produced for the isolated protactinium mixture at each of the time steps generated using the ORIGEN2 simulations. An example of this can be seen inFigure 9 for the PWRUS at 0 days and 300 days. Only protactinium isotopes were present at 0 days due to the lack of decay products. The gamma spectra for the other time steps and other reactors can be seen in Appendix C.

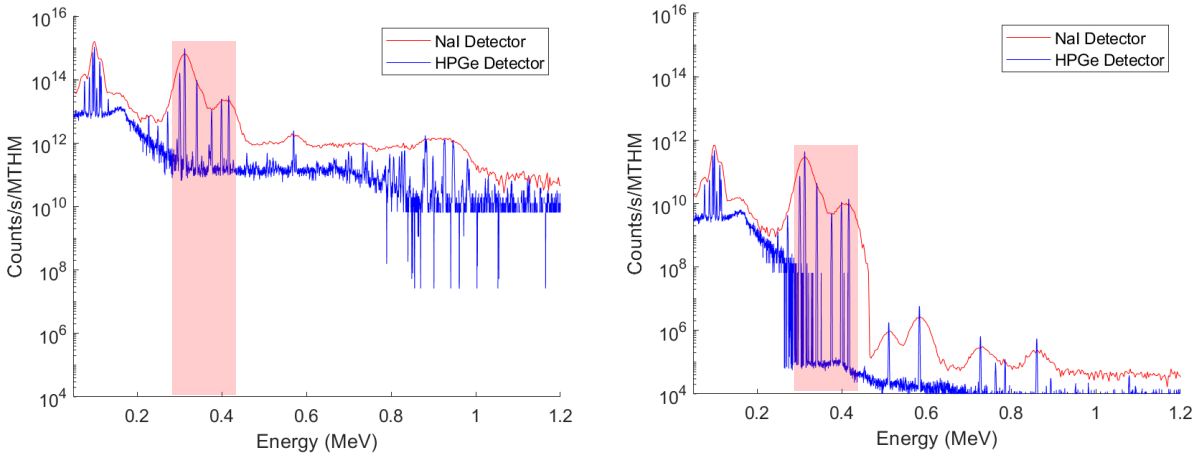

Figure 9: Gamma spectrum of the isotopes for the PWRUS reactor in the MCNP/ORIGEN2 simulations at time of discharge (left) and after 300 days (right). This gamma spectrum was produced using both a NaI detector (red) and a HPGe detector (blue) in MCNP. Relevant ^{233}Pa peaks are highlighted in the red boxes.

MCNP Burnup

The next step in the research was to simulate the burnup of a PWR and two CANDU reactors using MCNP. The PWR was modeled as a single fuel rod, shown in Figure 10, with mirrored boundaries to create an

infinite array of fuel rods. The modeled dioxide fuel had an actinide content of 80% Th and 20% U, with the uranium being 19.7% enriched. The fuel was burned for 1150 full power days with the following sequential time steps in days: 0.1, 0.2, 0.4, 0.5, 0.8, 1, 2, 4, 8, 16, 25, 50, 75, 100, 100, 100, 100, 100, 100, 100, 100, 167. The fuel and gap temperatures were modeled at 900 K and the cladding and water at 600 K. The neutron light water moderation treatment was used for the water, and its density was adjusted to 0.717 g/cm^3 to account for the elevated temperature and pressure of PWR primary coolant. K-code simulations were performed with 1000 particles per cycle for 2000 cycles, excluding results from the first 50 cycles due to potential biasing in neutron starting locations.

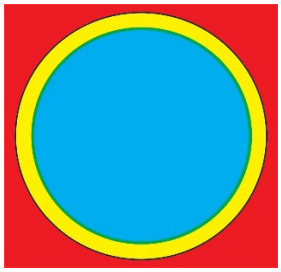

Figure 10: Axial view of the modeled PWR fuel rod. The fuel region is shown in blue, surrounded by a thin helium gap (green) followed by the zircaloy-4 cladding (yellow), which is surrounded by light water (red).

Both CANDU reactors were modeled as single fuel assemblies with mirrored boundaries, as shown in Figure 11. The first CANDU used U-Th-O_2 fuel with natural uranium and 19% of the fuel's actinide content being thorium. The second CANDU model used U-Th-O_2 fuel with 19.7% enriched uranium and 91% of the fuel's actinide content being thorium. The fuel was burned for 365 full power days with the following time steps in days: 0.1, 0.2, 0.4, 0.5, 0.8, 1, 2, 4, 8, 16, 25, 50, 75, 91, 91. The temperatures were the same as the PWR model, and the neutron heavy water moderation treatment was used for the water. The heavy water had a density of 0.836 g/cm^3 to account for the elevated temperature and pressure of CANDU. K-code simulation parameters were the same as those for the PWR simulations.

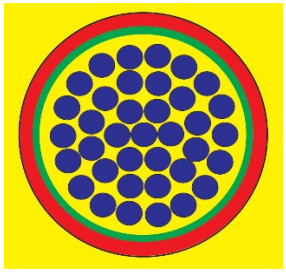

Figure 11: Axial view of the modeled CANDU fuel assembly. The fuel region is shown in blue, surrounded by a the Zircaloy-4 cladding (black), which is surrounded by heavy water (yellow). These fuel rods and coolant are encased in a cylindrical pressure tube of Zircaloy-4 (green), followed by a thin helium gap (not shown), then a cylindrical calandria tube of Zircaloy-4 (red), all surrounded by heavy water (yellow).

The gamma spectra for the generated protactinium isotopes and their decay products for each reactor were then produced for the same decay time steps as the previous simulations (0, 0.1, 1, 3, 10, 30, 100, and 300 days). Figure 12 shows the gamma spectrum for the extracted elemental protactinium from the PWR at 0 days and 300 days. The gamma spectra for the other time steps and other reactor models for the MCNP simulations can be found in Appendix D.

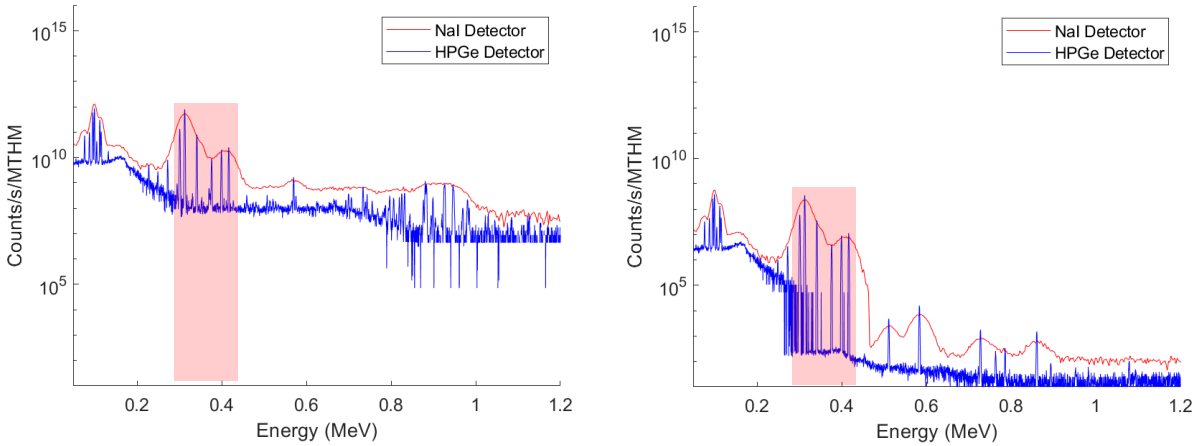

Figure 12: Gamma spectrum of the isotopes for the PWR using the MCNP stand-alone simulation at time of discharge (left) and after 300 days (right). This gamma spectrum was produced using both a NaI detector (red) and a HPGe detector (blue) in MCNP. Relevant ^{233}Pa peaks are highlighted in the red boxes.

SCALE/TRITON*

Since MSRs are often researched for thorium-fuel applications, and some designs include protactinium separation as part of online fuel processing, the nuclear industry and the international safeguards regime would benefit from evaluating the proliferation concerns for this type of reactor, including ^{233}Pa material accountancy. MSRs using liquid fuel require more complex modeling and simulation than PWRs and CANDU reactors due to the fact that the fuel is continuously flowing though the core region. Because of this, the TRITON sequence of the in-development beta version 16 of SCALE 6.3 was used to allow for continuous flow of the fuel in the MSR.

Core Design and Neutronics Modeling

Because its design specifications are available, the SD-TMSR design was chosen as the representative MSR core [44] with simulated continuous online reprocessing and refueling. This reactor is designed to be a single-fluid double-zone thorium-based molten salt reactor. The active core of this reactor has two main radial regions—the inner zone and the outer zone—in a hexagonal graphite matrix, as shown in Figure 13. The inner zone is composed of 486 relatively small fuel channels (3.5 cm radius) and the outer zone is composed of 522 larger fuel channels (5 cm radius). The two regions have the same channel pitch, which results in different fuel-to-moderator ratios in the two regions and allows for control over the breeding performance of the design. The core is designed to have a radial graphite reflector and surrounding cylindrical B_4C shielding and Hastelloy containments; however, these regions were modeled as a single hexagonal graphite region extending 48.65 cm beyond the active region.

The fuel salt is modeled as a lithium-beryllium fluoride salt carrying ^{232}Th and ^{233}U and with 100% ^{7}Li purity. The initial fuel salt composition of LiF-BeF_2-Th F_4-$^{233}UF_4$ was modeled as 70-17.5-12.3-0.2 mol% (about 44% ^{232}Th and 0.78% ^{233}U by weight). The first 1500 days of operation of the reactor were modeled, during which it was to maintain a specific power of 52.711 MW/MTHM. During the simulation, the active region had material flows designed to model the removal of material through reprocessing and the reintroduction of new fuel material. The flows were constructed to remove fission products and non-

* SCALE (standardized computer analyses for licensing evaluation) computer software developed at Oak Ridge National Laboratory is widely used and accepted around the world for many radiation transport applications. TRITON (transport rigor implemented with time-dependent operation for neutronic depletion) is a control module developed within the SCALE framework that enables 2-D and 3-D depletion calculations to be performed.

dissolved metals at a rate of 3.333 x 10^{-2} s^{-1} and actinides at a rate of 1.092 x 10^{-6} s^{-1}. Protactinium was also removed to a separate tank at a rate of 1.092 x 10^{-6} s^{-1}. ^{232}Th and ^{233}U were added back into the system at net rates normalized to the initial core inventory in kg-HM. During the first 90 days of operation the normalized net rates of ^{232}Th and ^{233}U were 2.02083 x 10^{-6} g/s and 1.42130 x 10^{-6} g/s, respectively. For the remaining simulation time, these rates were adjusted to 1.55015 x 10^{-6} g/s and 2.9375 x 10^{-6} g/s.

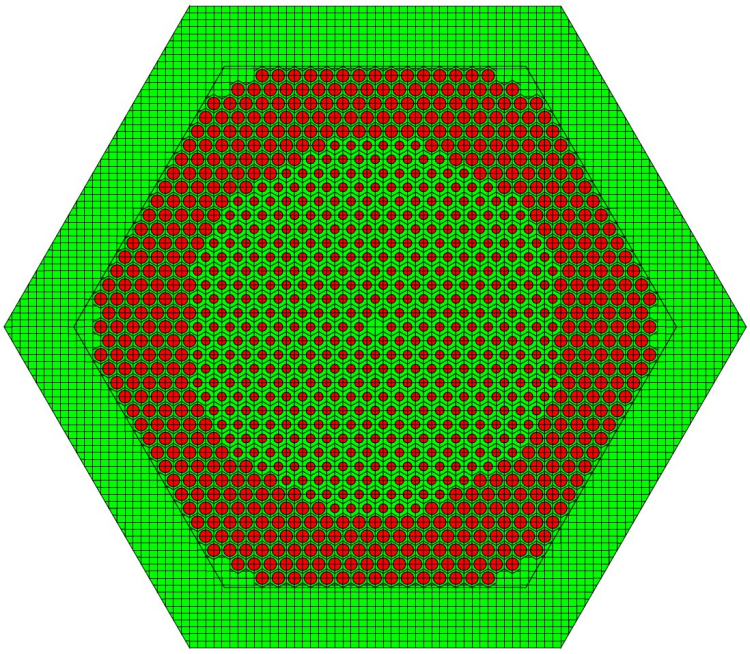

Figure 13: Modeled MSR reactor showing the fuel region (red) and graphite moderator (green).

Depletion and Material Source Term Modeling

In order to get a more detailed composition for the protactinium in the decay tank, further modeling was done using standalone ORIGEN-S with the depletion library created in the neutronics simulation. This required a two-step modeling process. In the first step, the reactor fuel composition was calculated using the same initial composition, material removal rates, and new fuel feed rates, but with much shorter time steps. From this, the protactinium isotope concentrations in the core were found and, with the removal rates of protactinium modeled, the rate at which each of the isotopes would be expected to enter the decay tank at each time. In the second step, the protactinium isotopes are modeled to flow into an initially empty tank with stepwise constant flow rates equal to the average flow rate for that time step. In the tank, the protactinium is allowed to decay over the 1500 days, modeled with zero incident flux and all non-protactinium nuclides assumed to be removed. The mass concentration for ^{232}Pa, ^{233}Pa, and ^{234}Pa in the tank can be seen in Figure 14.

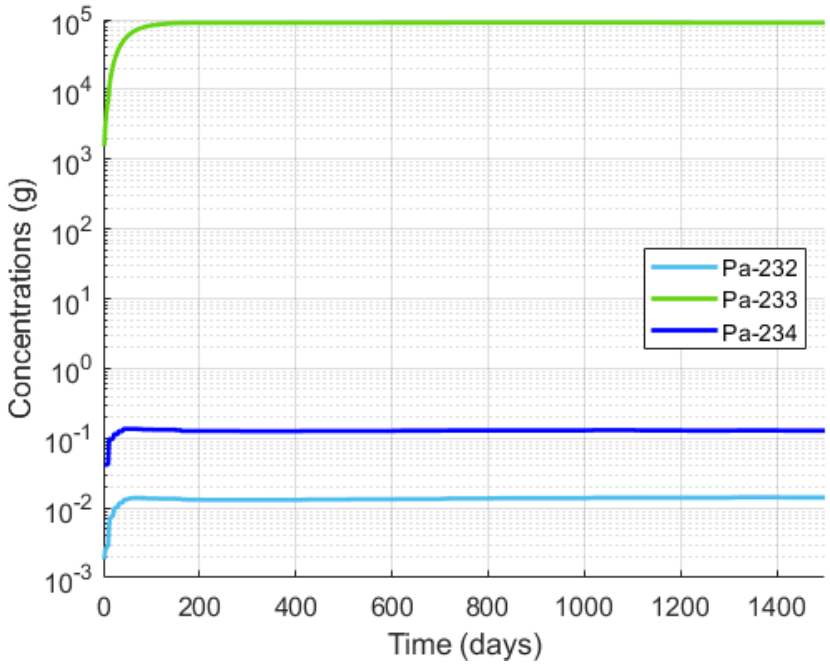

Figure 14: Mass concentration for ^{232}Pa, ^{233}Pa, and ^{234}Pa in the tank over time.

The gamma spectra from the separated elemental protactinium in the tank were produced for the MSR at 2, 10, 30, 100, and 300 days. The gamma spectra for 2 days and 300 days are shown below in Figure 15. The other time steps can be seen in Appendix E.

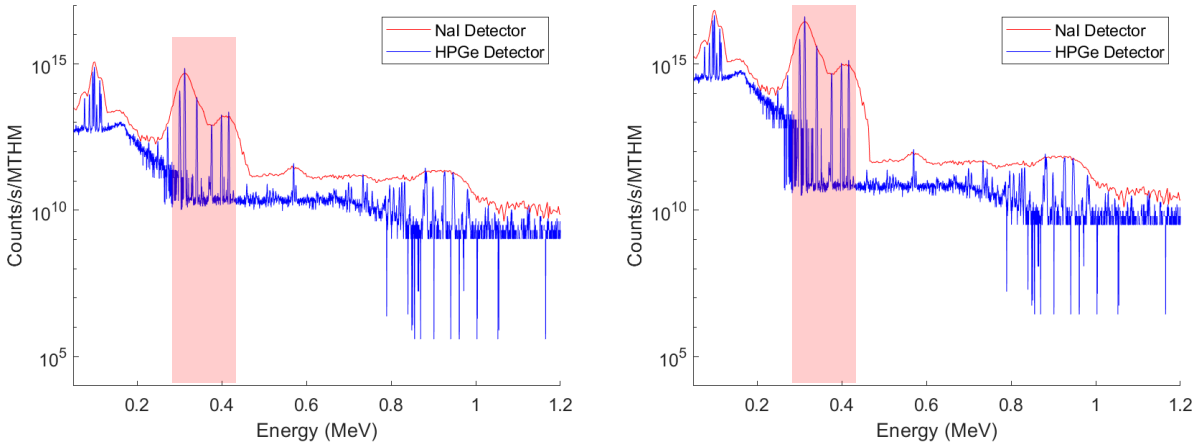

Figure 15: Gamma spectrum of the protactinium in the tank for the MSR using SCALE/TRITON simulation after 2 days (left) and after 300 days (right). This gamma spectrum was produced using both a NaI detector (red) and a HPGe detector (blue) in MCNP. Relevant ^{233}Pa peaks are highlighted in the red boxes.

DISCUSSION

Multiple DA and NDA techniques were reviewed and considered for their ability to measure ^{233}Pa in an extracted stream of elemental protactinium. This review identified HKED and passive gamma spectroscopy as potentially viable techniques that produce timely measurements. Due to the limited scope of this work, however, only passive gamma spectroscopy was evaluated. The spectra shown in Appendix A indicate that both NaI and HPGe detectors can easily identify ^{232}Pa and ^{233}Pa in isotopically pure samples under ideal conditions. The identification of ^{234}Pa may be more challenging due to fewer prominent gamma rays (as shown in Figure A3).

Because separating isotopically pure samples of protactinium from used fuel is unrealistic, several different reactor types were modeled to generate realistic compositions of the protactinium isotopes. This data, shown in Appendix B, indicate that the protactinium concentrations and compositions at the end of the fuel life for the PWR models are largely independent of slight differences in the neutron flux energy. For the CANDU models, the protactinium mass values show more variation than the PWR data, but are still mostly similar to each other. This indicates that the initial fraction of the fuel that is thorium and the initial enrichment of uranium has minimal impact on the protactinium mass values at the end of fuel life. This is likely due to the fact that all isotopes of protactinium have relatively short half-lives and thus do not continuously build up in the used fuel. When the PWRUS and CANDUSEU models (both of which use ~20% enriched uranium, with most of their initial actinide mass being thorium) are compared, there is a noticeable difference in the protactinium masses. The CANDU reactor produces about 10% less ^{232}Pa than the PWR. This is not surprising, since it is known that the concentration of ^{232}U in thorium fuel cycles has a slight dependence on the neutron energy spectrum of the reactor [45].

Gamma spectra were produced using the PWR and CANDU protactinium mass data described above. These gamma spectra can be found in Appendix C for the ORIGEN2 burnup simulations and Appendix D for the MCNP burnup simulations. For all simulated decay times, the data show how the cluster of ^{233}Pa gamma peaks in the 300–400 keV region remain visible for both NaI and HPGe detectors. The intensities of these peaks do decrease with decay time due to the relatively short half-life of ^{233}Pa. At zero days (extracting the protactinium from the used fuel immediately after it is discharged from the reactor), the counts from these peaks are approximately 10^{15} counts/s/MTHM/channel for the simulated measurement geometry. This value decreases to approximately 10^{12} counts/s/MTHM/channel after 300 days of decay. There is a lower-intensity cluster of peaks in the 800–1000 keV region that is visible at zero days. These peaks are due to other protactinium isotopes and rapidly drop in intensity with time, likely below detectable limits, due to the shorter half-lives of these isotopes. The unrealistically high count rates of these simulations should not be of concern, since the detector simulations used a very simple geometry. In a real measurement sample, self-shielding will attenuate some of the gamma rays and there will likely be more shielding and distance between the sample and detector. These differences between model and reality indicate the direction of follow-on research.

When comparing the ORIGEN2 burnup simulations to the MCNP burnup simulations, very few differences in the shape of the spectra are discernible for any of the reactor types. Given that ORIGEN2 uses significantly older data, this implies that the assumptions made by the two codes have minimal effect on the generated gamma spectra from the extracted protactinium. The results from the MSR simulations, shown in Appendix E, indicate that the gamma spectra are similar to those of other reactor types for the first few days of the simulation. However, rather than leaving the protactinium isotopes to decay as in the PWR and CANDU reactors, the MSR periodically extracts the protactinium from the fuel to add to the tank. This allows for all the protactinium isotope quantities to increase before approaching equilibrium (between 100 and 300 days, as shown in Figure 14). If an MSR design uses a batch process in which all material in

the tank is processed at once and the tank subsequently emptied and allowed to refill again, the gamma spectra could look substantially different because the protactinium isotopes would not be allowed to reach equilibrium. With MSRs still being designed, it is not known if MSR designs with online fuel processing will implement a continuous or batch approach with protactinium tank processing. Engaging with MSR designers would help researchers refine appropriate assumptions regarding continuous versus batch operations.

CONCLUSION

Thorium has been suggested as a nuclear fuel alternative, and many countries have shown interest in its use. It can be implemented in many traditional reactor designs as well as some yet-to-be built designs. This study focused on one potential proliferation pathway of thorium-fueled nuclear reactors: diversion of ^{233}Pa, which beta decays to become weapons-usable ^{233}U. Certain detection and measurement methods can be used to determine the quantity of ^{233}Pa in the fuel. While many previous studies have identified potential challenges and solutions, including highlighting DA and NDA techniques of potential use [13], the work presented here starts to quantify these challenges and solutions.

For the protactinium extraction time steps reported in this paper, ^{233}Pa was identified in isolated protactinium mixtures (with respective daughter products). However, more aspects must be considered, such as identification limitations within the reactor facility, protactinium isolation methods, evaluation of HKED capabilities, and additional material quantification for safeguards purposes, to name a few. This research assumes a best-case scenario of the protactinium detection. Each isotope was simulated as an unattenuated point source, which does not fully represent the geometry the protactinium material will be in. To better account for real world conditions, one would have to take into consideration self-shielding, attenuation from surrounding shielding, and gamma background created by nearby radioactive materials. Another factor to consider is that as time goes on, extracted ^{233}Pa will continue to decay, diminishing its quantity and making it more difficult to detect. With some reactor designs utilizing online processing, proliferators may then be able to conduct protracted diversions without being detected, allowing for the unmonitored collection of ^{233}Pa and subsequent production of ^{233}U. As NMA technologies continue to develop, other DA and NDA methods can be investigated and evaluated for ^{233}Pa detection and measurement. Results of this study show that detecting the presence and accounting for the quantity of ^{233}Pa in thorium-fueled reactor facilities seems to be an achievable goal. Considering the potential proliferation pathway of thorium-generated ^{233}Pa for the unsafeguarded production of ^{233}U, it would be prudent to monitor the production and quantity of ^{233}Pa in all thorium-fueled reactors, although thorium fueled PWRs and PHWRs are less of a concern because their used fuel cannot be immediately processed as it leaves the reactor core, unlike MSRs. Just as the production of other special fissionable materials are reported, the potential for diversion and misuse of thorium-generated ^{233}Pa exists and should be included in future discussions of these types of advanced reactor designs.

REFERENCES

1 International Atomic Energy Agency (IAEA). 2005. *Thorium Fuel Cycle—Potential Benefits and Challenges*. IAEA-TECDOC-1450. https://www-pub.iaea.org/mtcd/publications/pdf/te_1450_web.pdf.

2 IAEA. 2002. *IAEA Safeguards Glossary: 2001 Edition*. https://www.iaea.org/sites/default/files/iaea_safeguards_glossary.pdf.

3 World Nuclear Association. 2020. "Thorium." Information Library. https://world-nuclear.org/information-library/current-and-future-generation/thorium.aspx.

4 World Nuclear Association. 2020. "What is uranium? how does it work?" Information Library. https://world-nuclear.org/information-library/nuclear-fuel-cycle/introduction/what-is-uranium-how-does-it-work.aspx.

5 Kovacic, D. N., L. G. Worrall, A. Worral, G. F. Flanagan, D. E. Holcomb, R. Bari, L. Cheng, D. Farley and M. Sternat. 2018. Safeguards Challenges for Molten Salt Reactors. Presented at INMM Annual Meeting, Baltimore, MD. https://www.osti.gov/servlets/purl/1474868.

6 World Nuclear Association. 2021. "Molten Salt Reactors." Information Library. https://world-nuclear.org/information-library/current-and-future-generation/molten-salt-reactors.aspx.

7 US Department of Energy Nuclear Energy Research Advisory Committee. Molten Salt Reactor. December 2002. http://www.ne.doe.gov/genIV/documents/gen_iv_roadmap.pdf.

8 IAEA. 2014. *International Safeguards in the Design of Nuclear Reactors*. http://www-pub.iaea.org/MTCD/Publications/PDF/Pub1669_web.pdf.

9 Worral, A., J. W. Bae, B. R. Betzler, S. Greenwood and L. G. Worrall. 2019. *Molten Salt Reactor Safeguards: The Necessity of Advanced Modeling and Simulation to Inform on Fundamental Signatures.* https://www.ornl.gov/sites/default/files/2020-05/PAPER%20-%20MSR%20Safeguards%20Challenges.pdf.

10 Uribe, E. C. 2018. *Protactinium Presents a Challenge for Safeguarding Thorium Reactors*. https://www.osti.gov/servlets/purl/1594642.

11 International Atomic Energy Agency. 1989. *Statute: As Amended Up to 28 December 1989*. https://www.iaea.org/sites/default/files/statute.pdf.

12 Worrall, A., B. Betzler, G. Flanagan, D. Holcomb, J. Hu, D. Kovacic, L. Qualls and L. Worrall. 2018. "Molten Salt Reactors and Associated Safeguards Challenges and Opportunities." in *IAEA Symposium on International Safeguards*. https://conferences.iaea.org/event/150/contributions/5423/contribution.pdf.

13 Swift, A., K. Hogue, T. Folk and J. Cooley. 2020. *Safeguards Technical Objectives for Thorium Molten Salt Reactor Fuel Cycles*. https://www.osti.gov/servlets/purl/1763719.

14 Lloyd, C. and B. Goddard. 2020. "Impact of Gamma Ray Emissions of Materials Containing 232U on Safety, Security, and Safeguards." *Nuclear Engineering and Design* 370: 110905. https://doi.org/10.1016/j.nucengdes.2020.110905.

15 Lloyd, C., B. Goddard and R. Witherspoon. 2019. "The effects of U-232 on enrichment and material attractiveness over time." *Nuclear Engineering and Design* 352: 110175. https://doi.org/10.1016/j.nucengdes.2019.110175.

16 Boulyga, S., S. Konegger-Kappel, S. Richter, and L. Sangely, 2015. "Mass spectrometric analysis for nuclear safeguards." *Journal of Analytical Atomic Spectrometry* 30 (7): 1469-1489. https://doi.org/10.1039/C4JA00491D.

17 Suzuki, D., F. Esaka, Y. Miyamoto, and M. Magara. 2014. "Direct isotope ratio analysis of individual uranium-plutonium mixed particles with various U/Pu ratios by thermal ionization mass spectrometry." *Applied Radiation and Isotopes* 96: 52-56. https://doi.org/10.1016/j.apradiso.2014.11.012.

18 Eppich, G. R., Z. Macsik, R. Katona, S. Konegger-Kappel, G. Stadelmann, A. Kopf, B. Varga, and S. Boulyga. 2019. "Plutonium assay and isotopic composition measurements in nuclear safeguards samples by inductively coupled plasma mass spectrometry." *Journal of Analytical Atomic Spectrometry* 34 (6):. 1154-1165. https://doi.org/10.1039/C9JA00047J.

19 Quemet, A., A. Ruas, V. Dalier and C. Rivier, "Development and comparison of high accuracy thermal ionization mass spectrometry methods for uranium isotope ratios determination in nuclear fuel." *International Journal of Mass Spectrometry*, vol. 438, pp. 166-174, 2019.

20 Wang, F., Y. Zhang, Y.-g. Zhao, D.-f. Guo, S.-k. Xie, J. Tan, J.-y. Li, and J. Lu. 2018. "Application of laser ionization mass spectrometry for measurement of uranium isotope ratio in nuclear forensics and nuclear safeguards." *Measurement Science and Technology* 29 (9): 095903. https://doi.org/10.1088/1361-6501/aad31e.

21 Coble, J. B., S. E. Skutnik, S. N. Gilliam, and M. P. Cooper. 2020. "Review of Candidate Techniques for Material Accountancy Measurements in Electrochemical Separations Facilities." *Nuclear Technology* 206 (12): 1803-1826. https://doi.org/10.1080/00295450.2020.1724728.

22 Varga, Z., M. Krachler, A. Nicholl, M. Ernstberger, T. Wiss, M. Wallenius, and K. Mayer. 2018. "Accurate measurement of uranium isotope ratios in solid samples by laser ablation multi-collector inductively coupled plasma mass spectrometry." *Journal of Analytical Atomic Spectrometry* 33 (6): 1076-1080. http://doi.org/10.1039/C8JA00006A.

23 Harvey, D. 2011. "Chapter 8: Gravimetric Methods." In *Analytical Chemistry 2.0*, 355-409. https://drive.google.com/file/d/1o7vXew3PysO3lAaaslvcsaj8f8f3P7Cg/view.

24 Braun, R. D. 2021. "Chemical analysis." In *Encyclopedia Britannica*. https://www.britannica.com/science/chemical-analysis.

25 Stewart, J. E. 1991."Principles of Total Neutron Counting." In *Passive Nondestructive Assay of Nuclear Materials*, edited by D. Reilly, N. Enselin, and H. Smith Jr., 407-434. https://www.lanl.gov/org/ddste/aldgs/sst-training/_assets/docs/PANDA/Principles%20of%20Neutron%20Counting%20Ch.%2014%20p.%20407-434.pdf.

26 DeSimone, D., A. Favalli, D. MacArthur, C. Moss and J. Thron. 2010. *Review of Active Interrogation Techniques and Considerations for Their Use behind an Information Barrier*. https://www.nti.org/wp-content/uploads/2021/09/LA-UR-10-06958_Rev_Active_Interrog_Techniques_Consid_Use_Info_Barrier.pdf

27 D.A. Brown, et. al., ENDF/B-VIII.0: The 8th Major Release of the Nuclear Reaction Data Library with CIELO-project Cross Sections, New Standards and Thermal Scattering Data, Nuclear Data Sheets, Volume 148, 2018, pp.1-142, ISSN 0090-3752.

28 *Application Note: KED/KXRF Hybrid Densitometer.* 1996. https://pdfslide.net/documents/kedkxrf-hybrid-hybrid-densitometer-employs-a-combin-ation-of-two-complementary.html.

29 Canberra. *International Nuclear Safeguards Solutions: Nuclear Measurement Solutions for Safety, Security, & the Environment*. 2017. https://www.mirion.com/assets/c40890_safeguards_brochure_jpQNo6N.pdf.

30 Williams, A. N. and S. Phongikaroon. 2017. "Laser-Induced Breakdown Spectroscopy (LIBS) in a Novel Molten Salt Aerosol System." *Applied Spectroscopy* 71 (4): 744-749. https://doi.org/10.1177%2F0003702816648965.

31 Hauck, D. K., D. S. Bracken, D. W. MacArthur, P. A. Santi and J. Thron. 2010. *Feasibility study on using fast calorimetry technique to measure a mass attribute as part of a treaty verification regime.* https://www.osti.gov/servlets/purl/1016119.

32 Croft, S., S. Phillips, L. G. Evans, J. Guerault, G. Jossens, L. Passelegue and C. Mathonat. 2010. Nuclear Calorimetry—Dispelling the Myths. Presented at WM2010 Conference, Phoenix, AZ. https://silo.tips/download/nuclear-calorimetry-dispelling-the-myths-s-croft-s-philips-lg-evans-j-guerault-g.

33 Cremers, L. and T. E. Sampson. 2010. Calorimetry of low mass Pu239 items. Presented at 2010 New Brunswick Laboratory Measurement Evaluation Program Meeting, Baltimore, MD. https://www.osti.gov/servlets/purl/1014455.

34 Rudy, C. R., D. S. Bracken, M. K. Smith and M. J. Schanfein. 2000. Calorimetry of TRU Waste Materials. Presented at Spectrum 2000 International Conference on Nuclear and Hazardous Waste Management, Chattanooga, TN. https://www.osti.gov/servlets/purl/768814.

35 Campbell, L. W., L. E. Smith, and A. C. Misner. 2011. "High-Energy Delayed Gamma Spectroscopy for Spent Nuclear Fuel Assay." *IEEE Transactions on Nuclear Science* 58 (1) 231-240. https://doi.org/10.1109/TNS.2010.2095039.

36 Gauld, I. C., and M. W. Francis. 2010. Investigation of Passive Gamma Spectroscopy to Verify Spent Nuclear Fuel Content. Presented at INMM 51st Annual Meeting, Baltimore, MD. https://www.osti.gov/biblio/993016.

37 Werner, C. J., J. S. Bull, C. J. Solomon, F. B. Brown, G. W. McKinney, M. E. Rising, D. A., Dixon, R. L. Martz, et al. 2018. *MCNP6.2 Release Notes*. https://doi.org/10.2172/1419730.

38 Hiller, L., T. Gosnell, J. Gronberg and D. Wright. 2013. *RadSrc Library and Application Manual*. https://nuclear.llnl.gov/simulation/radsrc_v1.6_doc/radsrc.pdf.

39 RSICC Computer Code CCC-371. 2021. Oak Ridge National Laboratory. https://rsicc.ornl.gov/codes/ccc/ccc3/ccc-371.html.

40 Croff, A. G. 1980. *A User's Manual for the ORIGEN2 Computer Code*. https://www.osti.gov/servlets/purl/5285077.

41 Rouben, B. 2003. *CANDU Fuel-Management Course*. https://canteach.candu.org/content%20library/20031101.pdf.

42 Trellue, H. R., C. G. Bathke and P. Sadasivan. 2011."Neutronics and material attractiveness for PWR thorium systems using Monte Carlo techniques." *Progress in Nuclear Energy* 53 (6) 698-707. http://dx.doi.org/10.1016/j.pnucene.2011.04.007.

43 Boczar, P. G., G. R. Dyck, P. S. W. Chan and D. B. Buss. 2002. "Recent advances in thorium fuel cycles for CANDU reactors." In *Thorium fuel utilization: Options and trends*, *Proceedings of three IAEA meetings held in Vienna in 1997, 1998 and 1999*. https://www-pub.iaea.org/MTCD/publications/PDF/te_1319_web.pdf.

44 Ashraf, O., A. Rykhlevskii, G. V. Tikhomirov, and K. D. Huff. 2020. "Whole core analysis of the single-fluid double-zone thorium molten salt reactor (SD-TMSR)." *Annals of Nuclear Energy* 137: 107115. https://doi.org/10.1016/j.anucene.2019.107115.

45 Kang, J. and F. Hippel. 2001."U-232 and the Proliferation Resistance of U-233 in Spent Fuel." *Science & Global Security* 9: 1-32. http://dx.doi.org/10.1080/08929880108426485.

Appendix A: GAMMA SPECTRA FOR 232PA, 233PA, AND 234PA

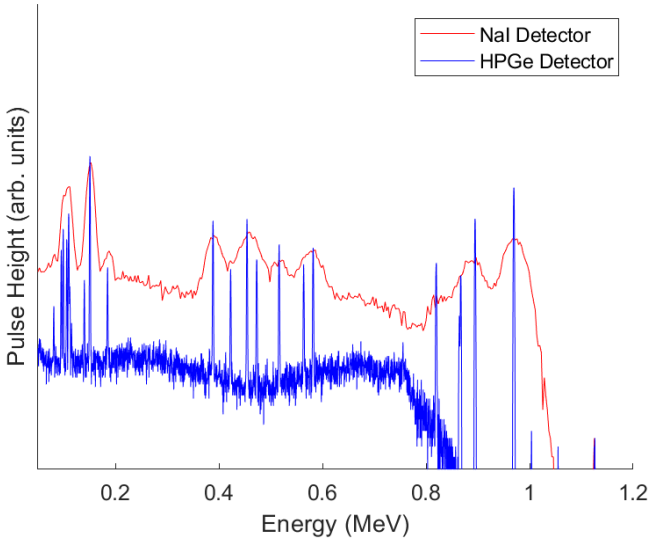

Figure A-1: ^{232}Pa gamma spectrum.

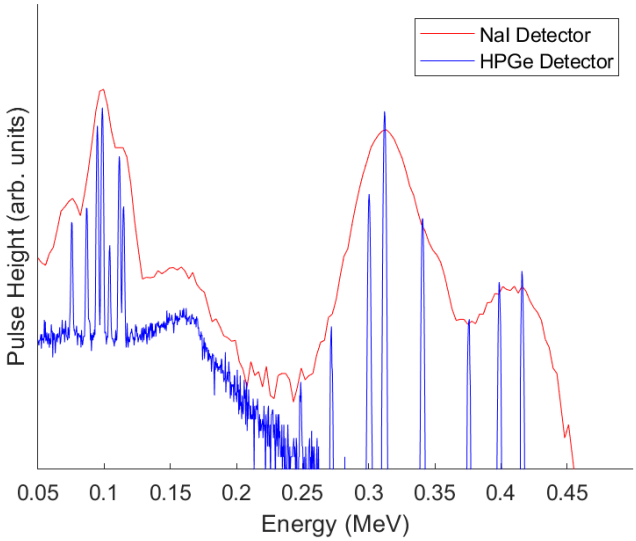

Figure A-2: ^{233}Pa gamma spectrum.

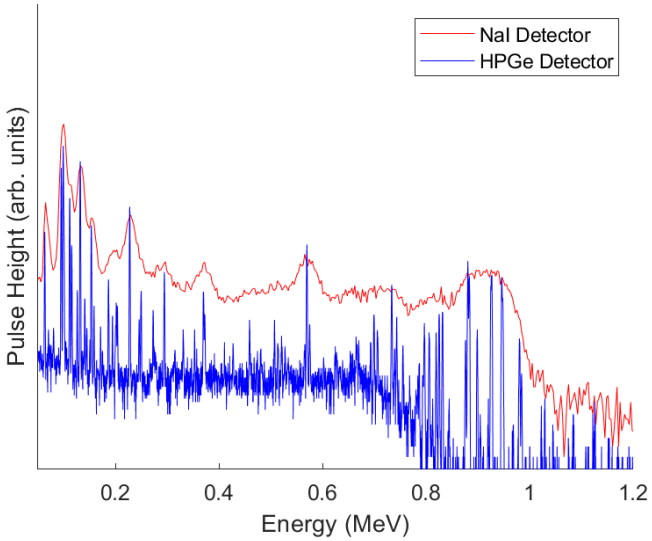

Figure A-3: ^{234}Pa gamma spectrum.

Appendix B: ORIGEN2 OUTPUT FOR PA AND U

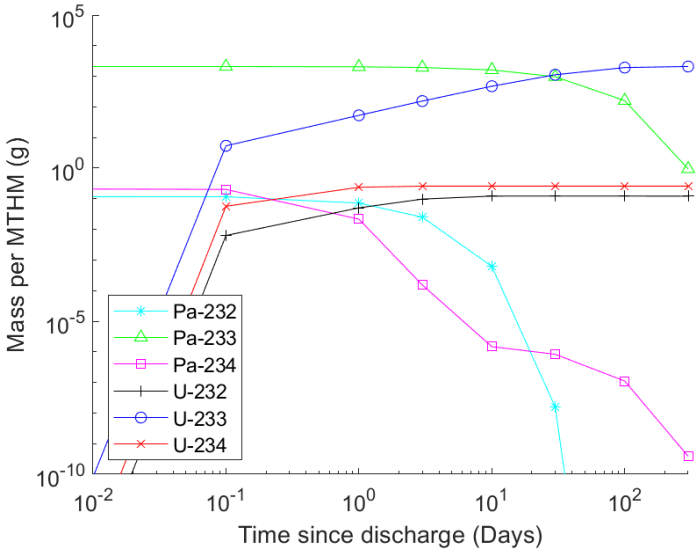

Figure B-1: Relative abundance of isotopes for PWRUS.

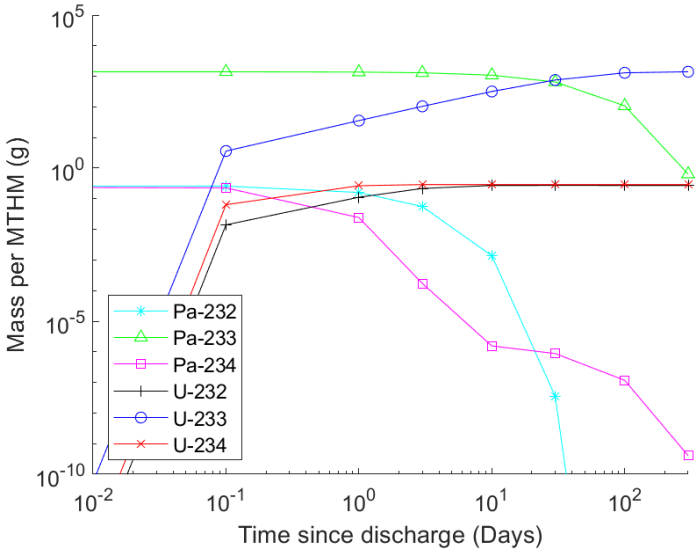

Figure B-2: Relative abundance of isotopes for PWRD5D35.

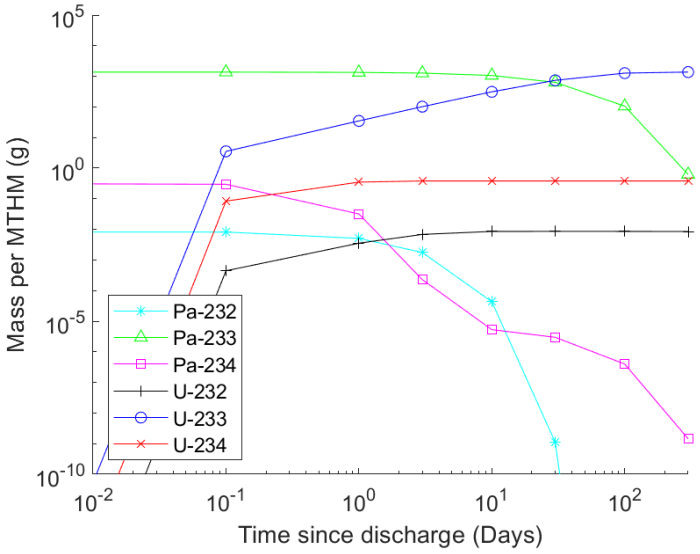

Figure B-3: Relative abundance of isotopes for CANDUNAU.

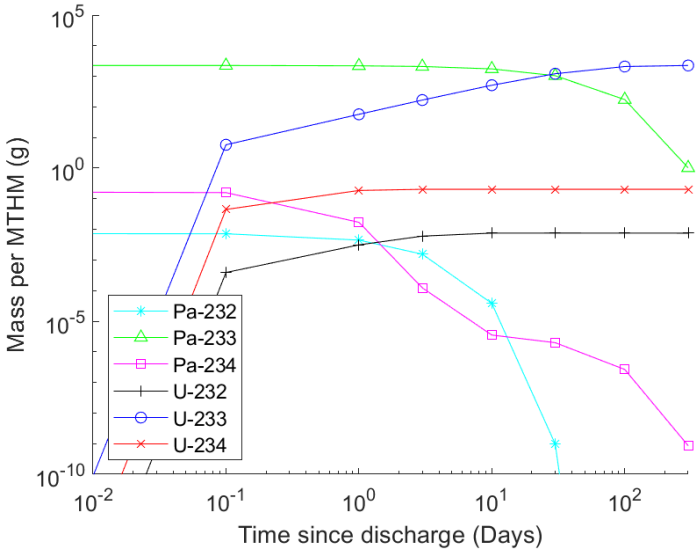

Figure B-4: Relative abundance of isotopes for CANDUSEU.

Appendix C: Gamma Spectra for Separated Protactinium Mixture for ORIGEN2 Burnup Simulations

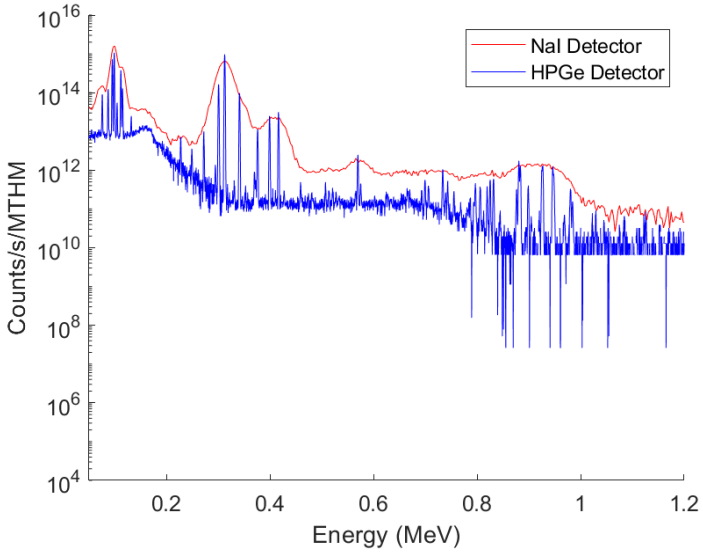

Figure C-1: Gamma spectrum for PWRUS at 0 days.

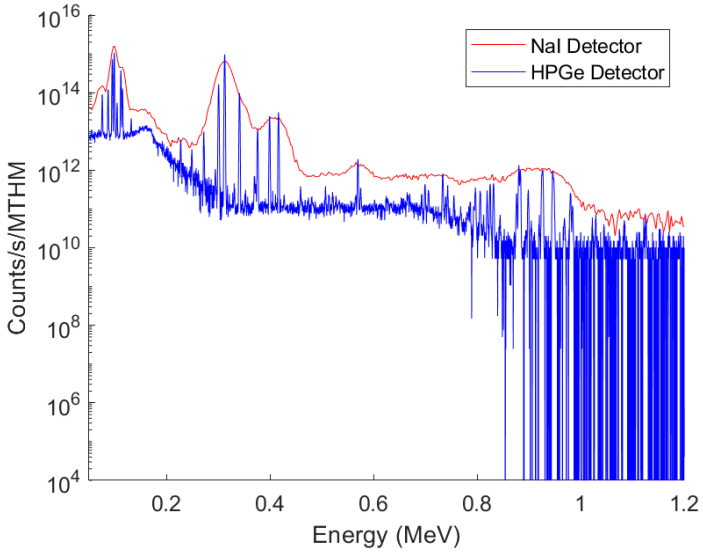

Figure C-2: Gamma spectrum for PWRUS at 0.1 days.

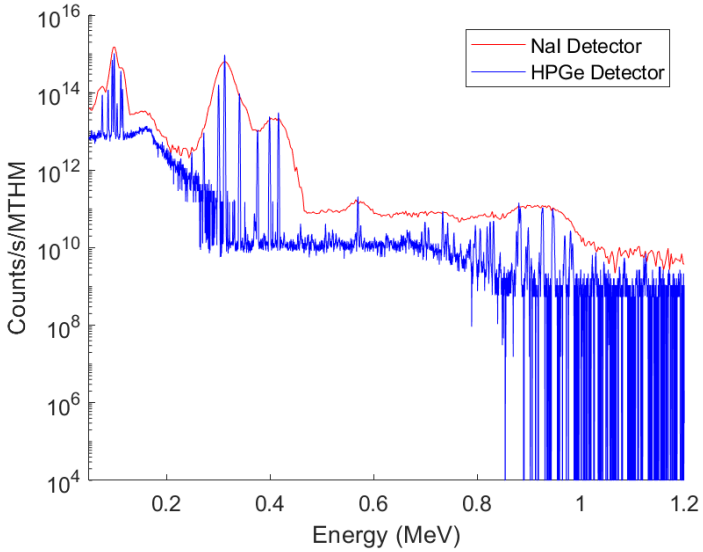

Figure C-3: Gamma spectrum for PWRUS at 1 day.

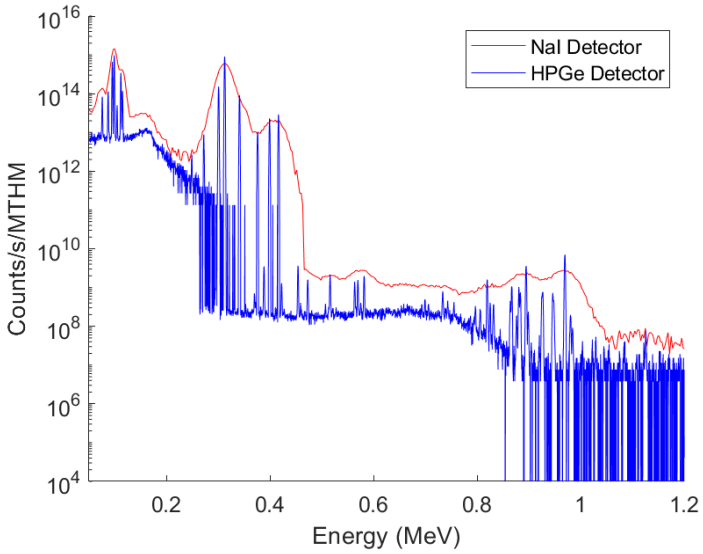

Figure C-4: Gamma spectrum for PWRUS at 3 days.

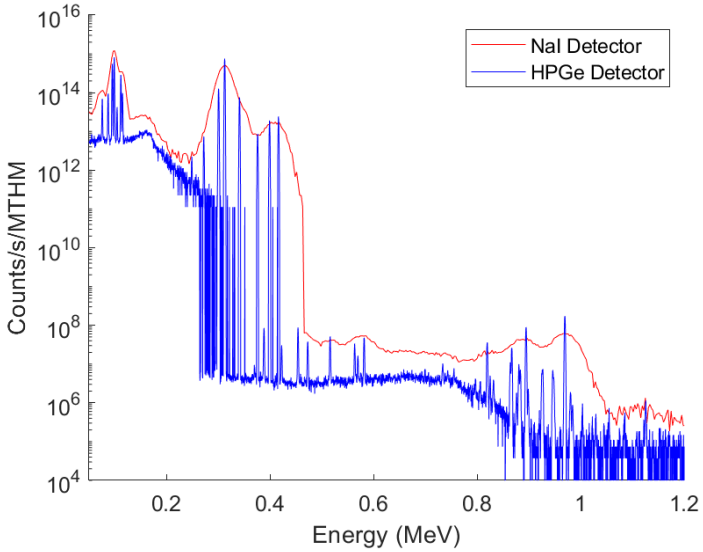

Figure C-5: Gamma spectrum for PWRUS at 10 days.

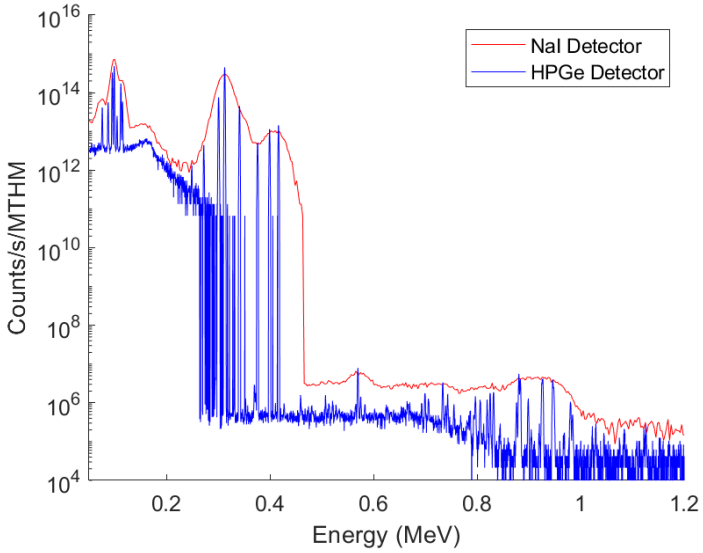

Figure C-6: Gamma spectrum for PWRUS at 30 days.

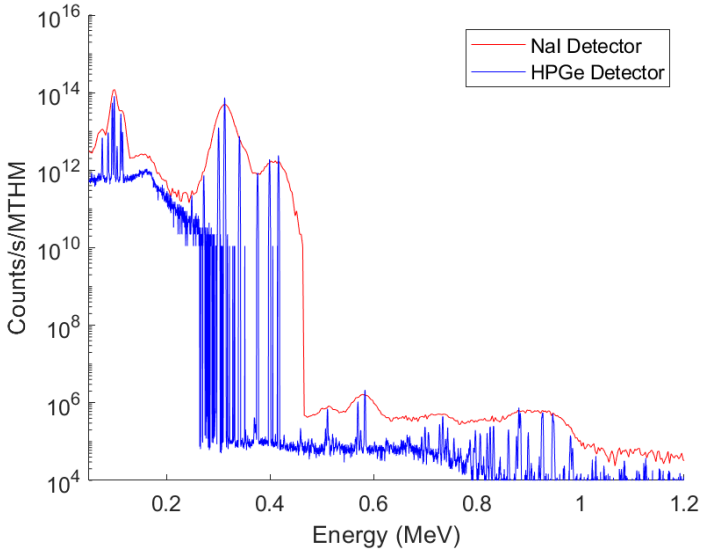

Figure C-7: Gamma spectrum for PWRUS at 100 days.

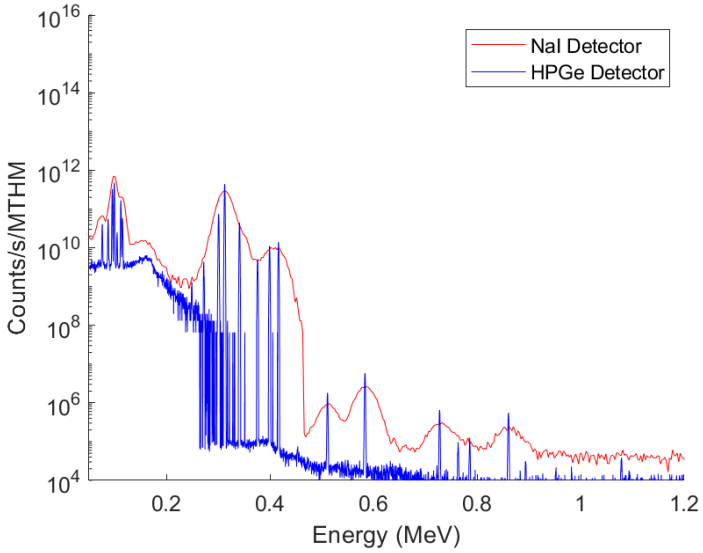

Figure C-8: Gamma spectrum for PWRUS at 300 days.

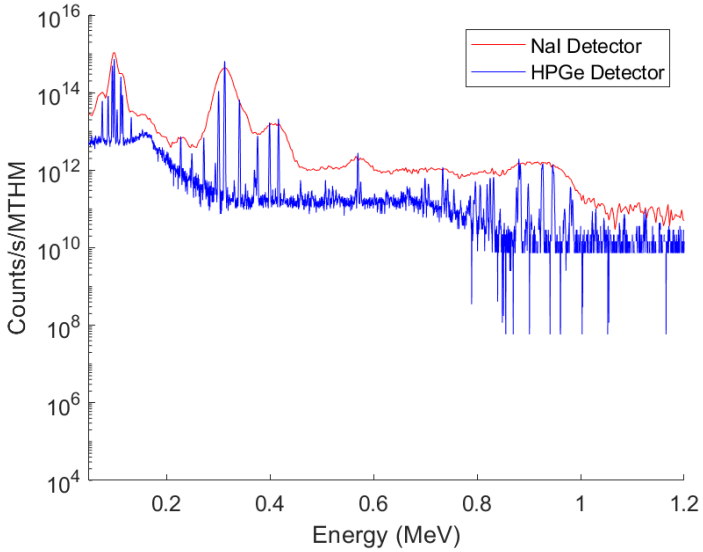

Figure C-9: Gamma spectrum for PWRD5D35 at 0 days.

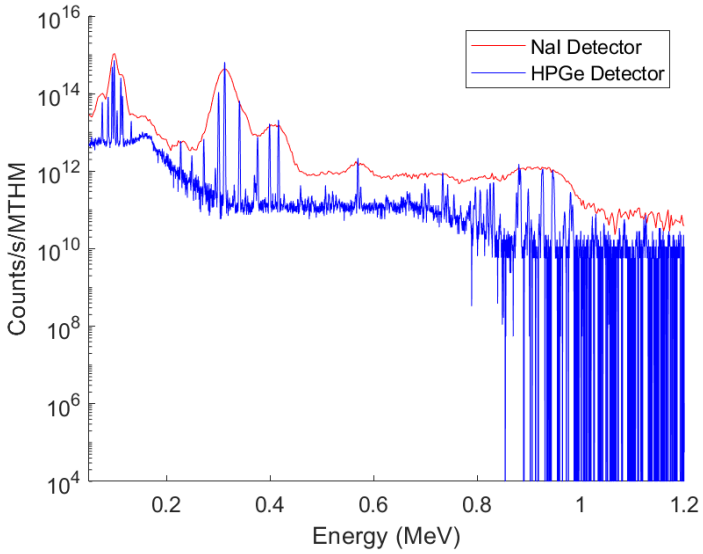

Figure C-10: Gamma spectrum for PWRD5D35 at 0.1 days.

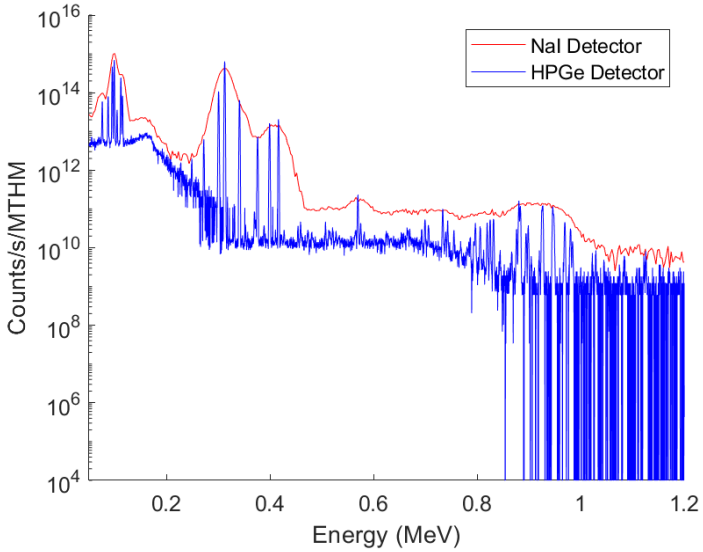

Figure C-11: Gamma spectrum for PWRD5D35 at 1 day.

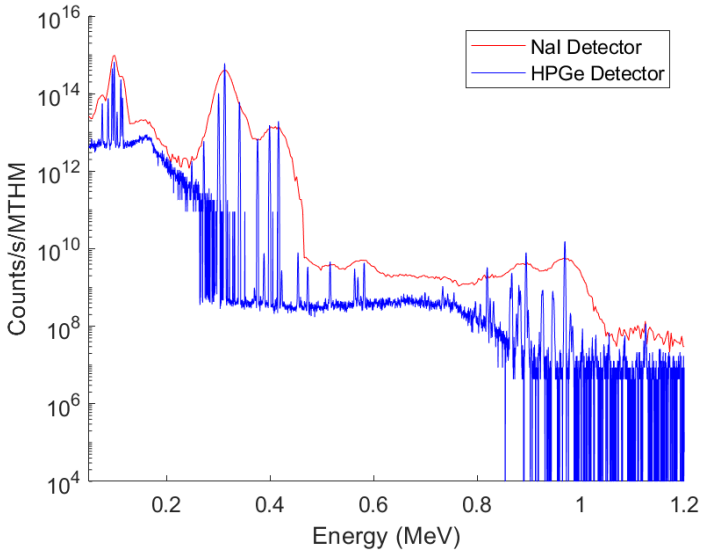

Figure C-12: Gamma spectrum for PWRD5D35 at 3 days.

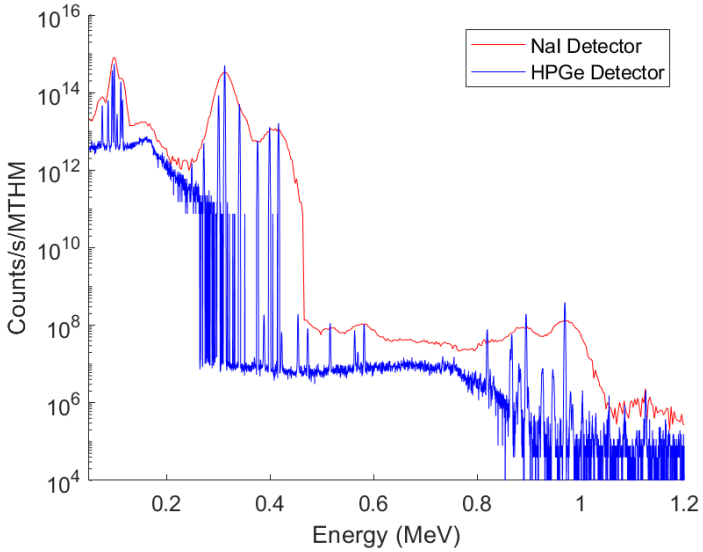

Figure C-13: Gamma spectrum for PWRD5D35 at 10 days.

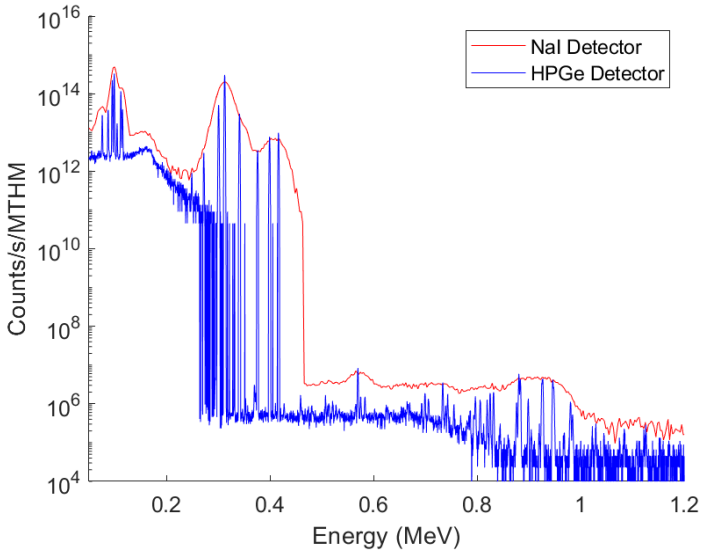

Figure C-14: Gamma spectrum for PWRD5D35 at 30 days.

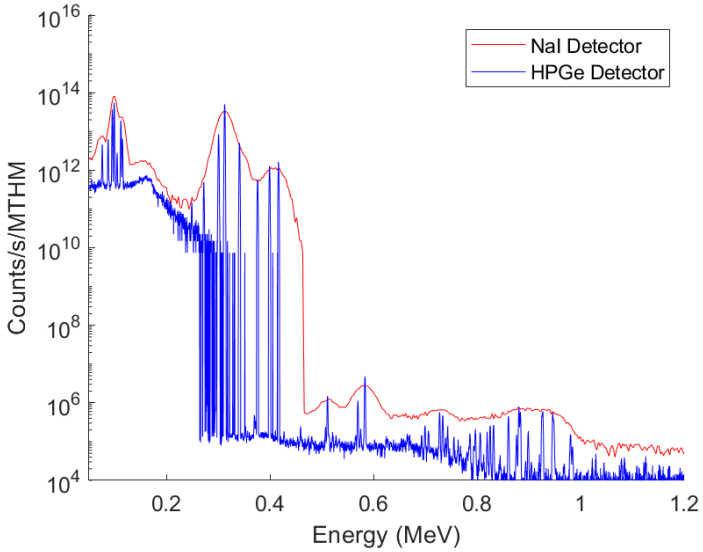

Figure C-15: Gamma spectrum for PWRD5D35 at 100 days.

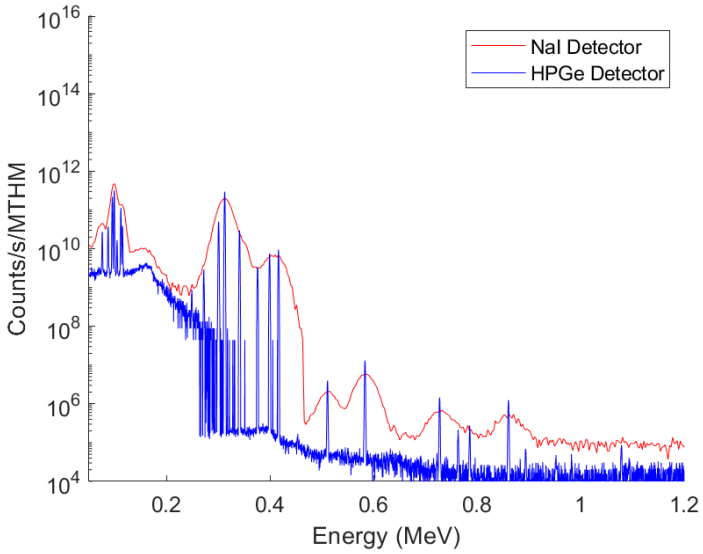

Figure C-16: Gamma spectrum for PWRD5D35 at 300 days.

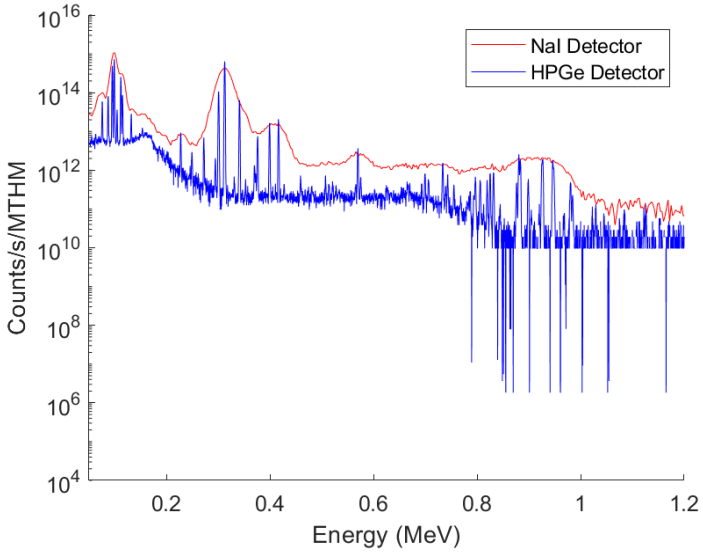

Figure C-17: Gamma spectrum for CANDUNAU at 0 days.

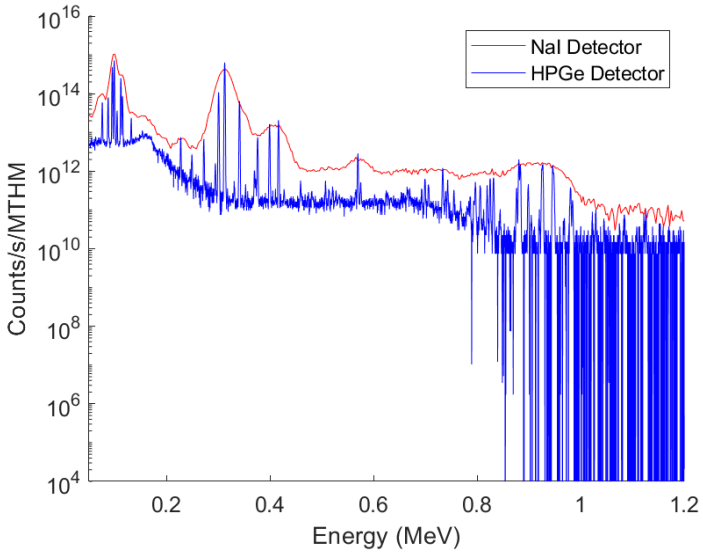

Figure C-18: Gamma spectrum for CANDUNAU at 0.1 days.

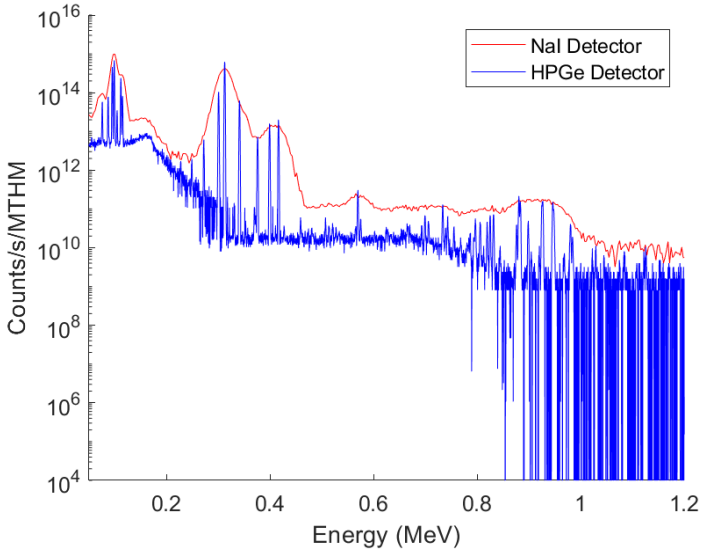

Figure C-19: Gamma spectrum for CANDUNAU at 1 day.

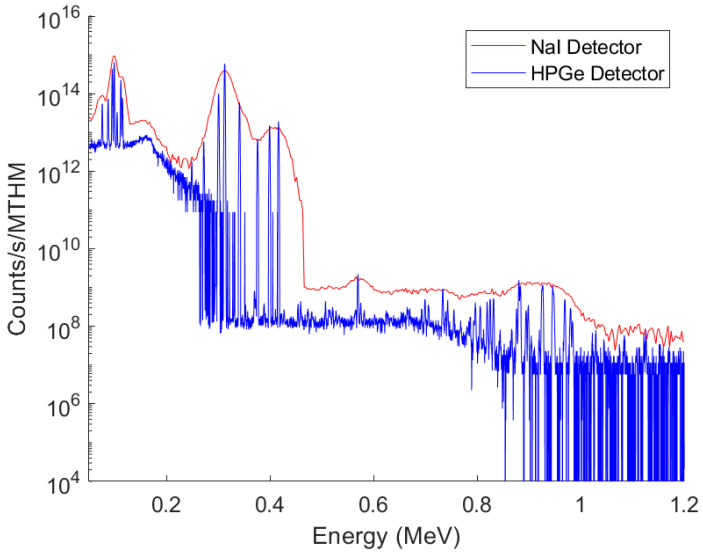

Figure C-20: Gamma spectrum for CANDUNAU at 3 days.

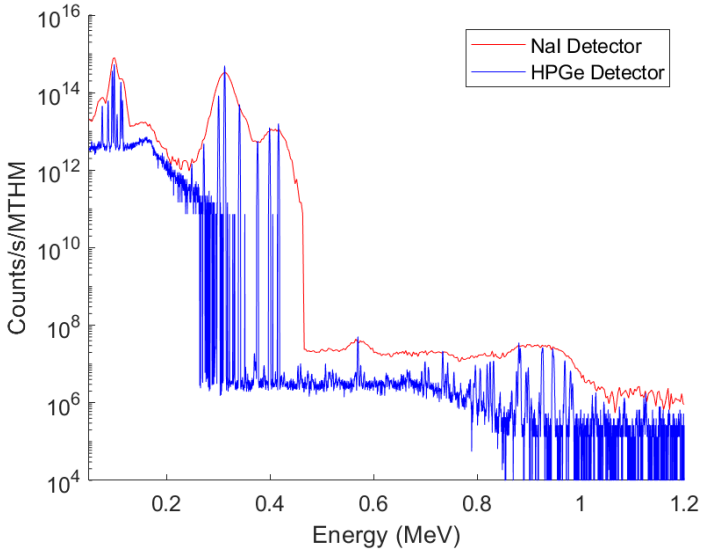

Figure C-21: Gamma spectrum for CANDUNAU at 10 days.

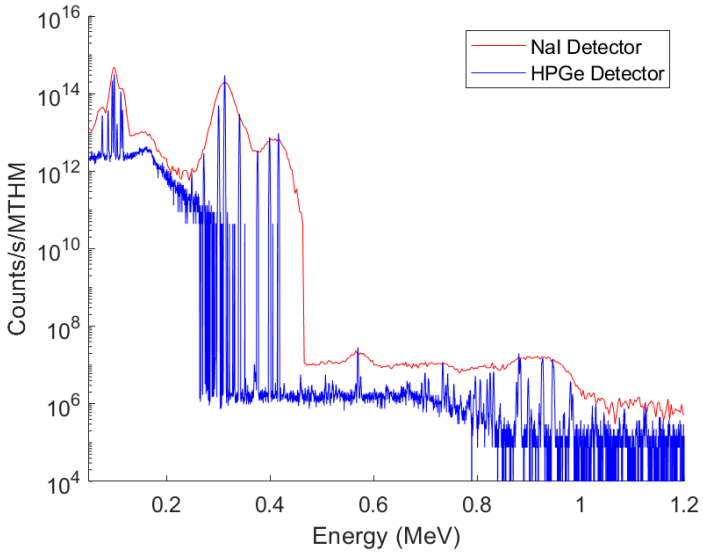

Figure C-22: Gamma spectrum for CANDUNAU at 30 days.

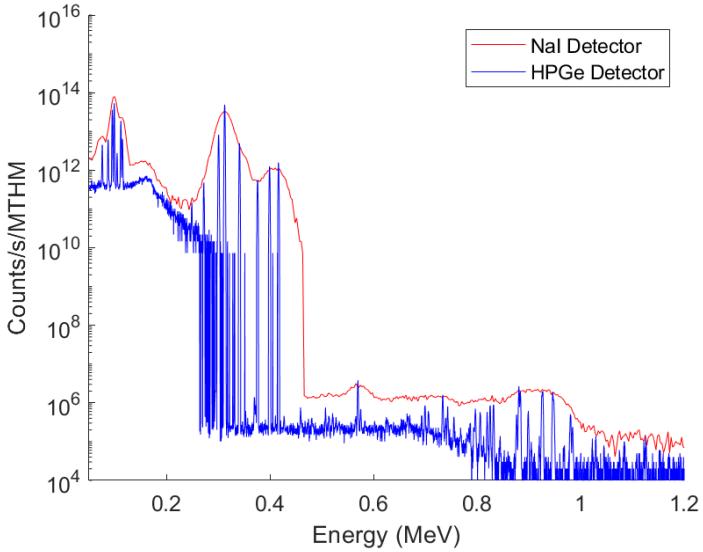

Figure C-23: Gamma spectrum for CANDUNAU at 100 days.

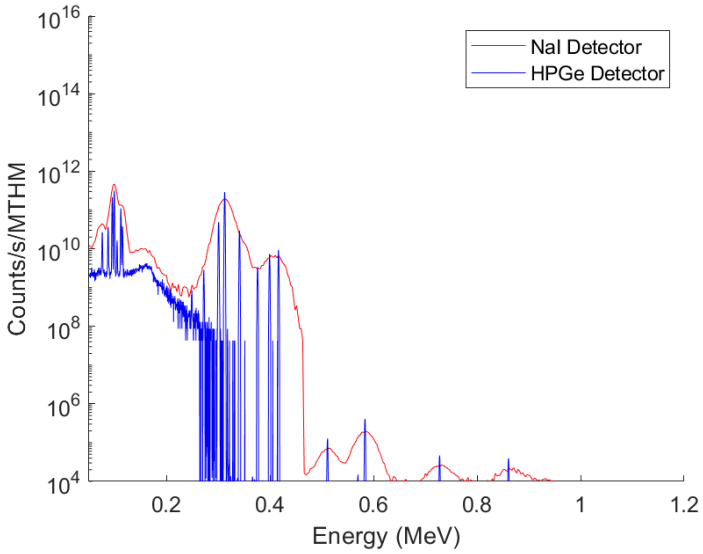

Figure C-24: Gamma spectrum for CANDUNAU at 300 days.

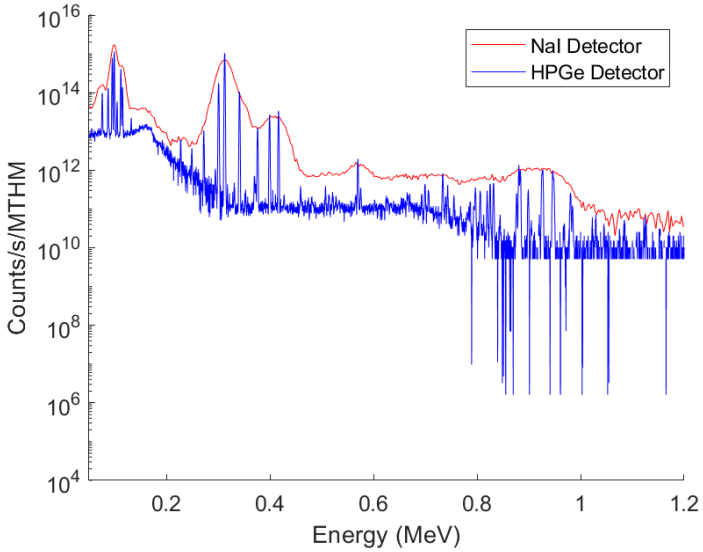

Figure C-25: Gamma spectrum for CANDUSEU at 0 days.

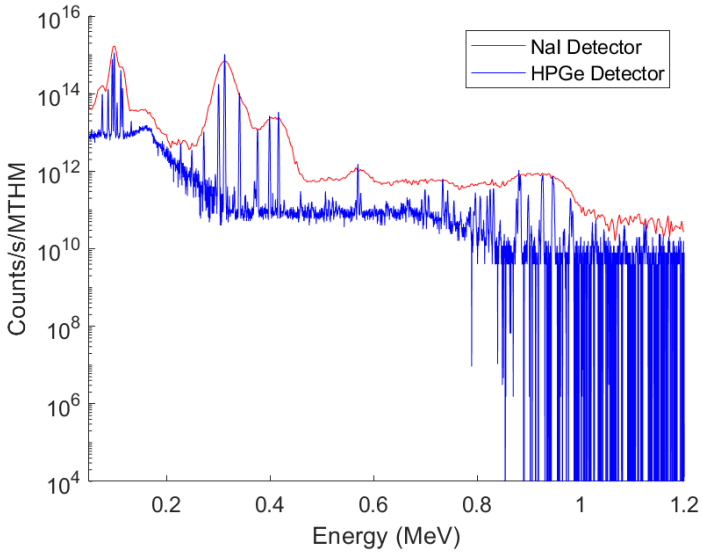

Figure C-26: Gamma spectrum for CANDUSEU at 0.1 days.

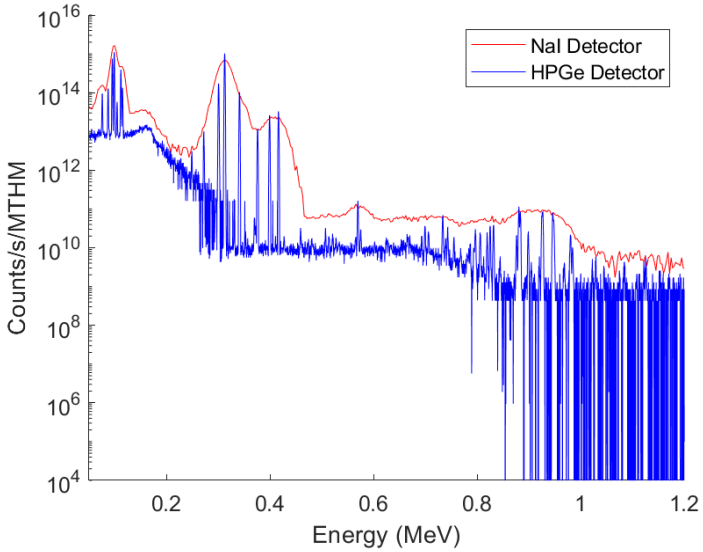

Figure C-27: Gamma spectrum for CANDUSEU at 1 day.

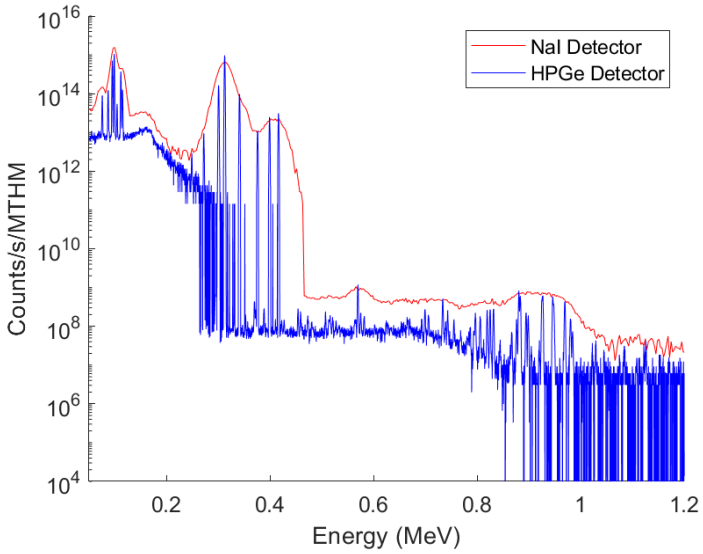

Figure C-28: Gamma spectrum for CANDUSEU at 3 days.

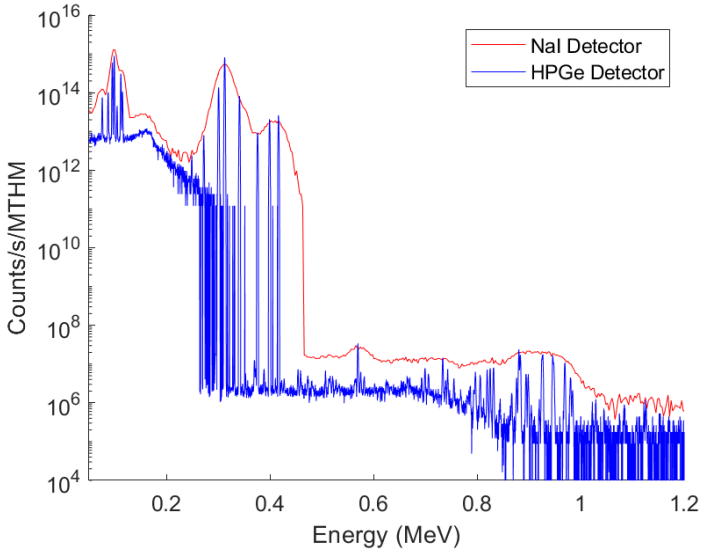

Figure C-29: Gamma spectrum for CANDUSEU at 10 days.

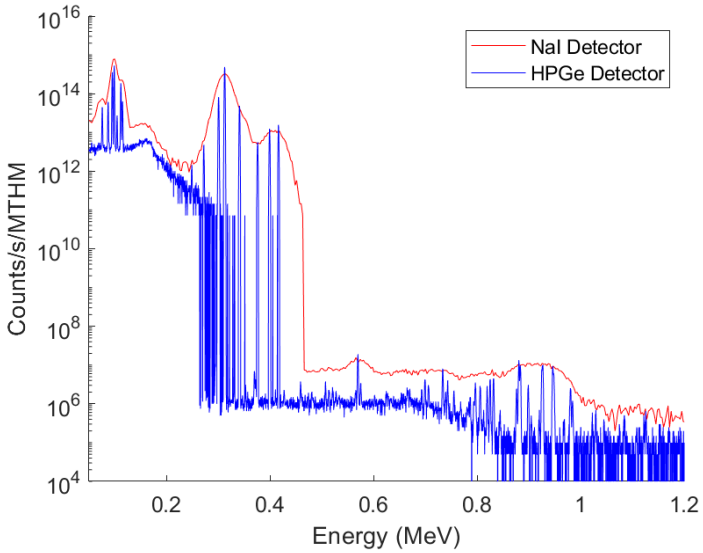

Figure C-30: Gamma spectrum for CANDUSEU at 30 days.

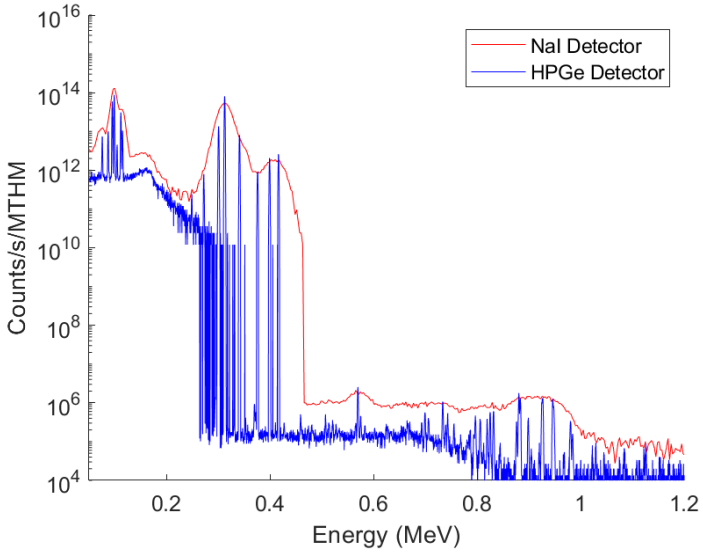

Figure C-31: Gamma spectrum for CANDUSEU at 100 days.

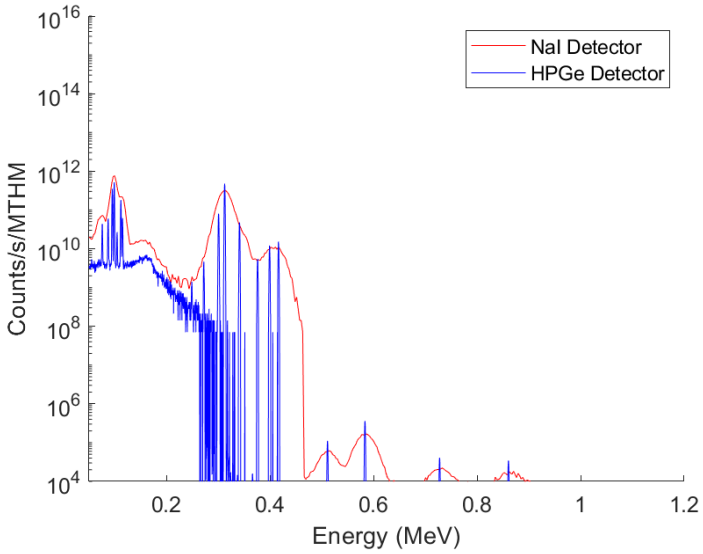

Figure C-32: Gamma spectrum for CANDUSEU at 300 days.

Appendix D: Gamma Spectra for Separated Protactinium Mixture for MCNP Burnup Simulations

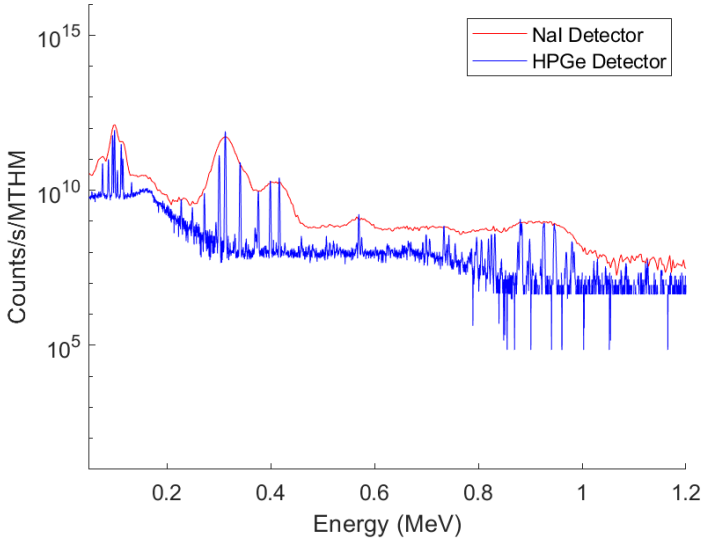

Figure D-1: Gamma spectrum for PWR at 0 days.

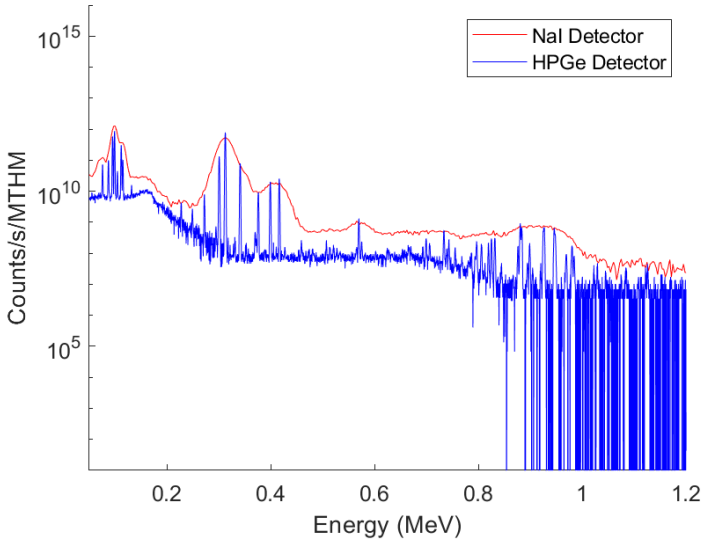

Figure D-2: Gamma spectrum for PWR at 0.1 days.

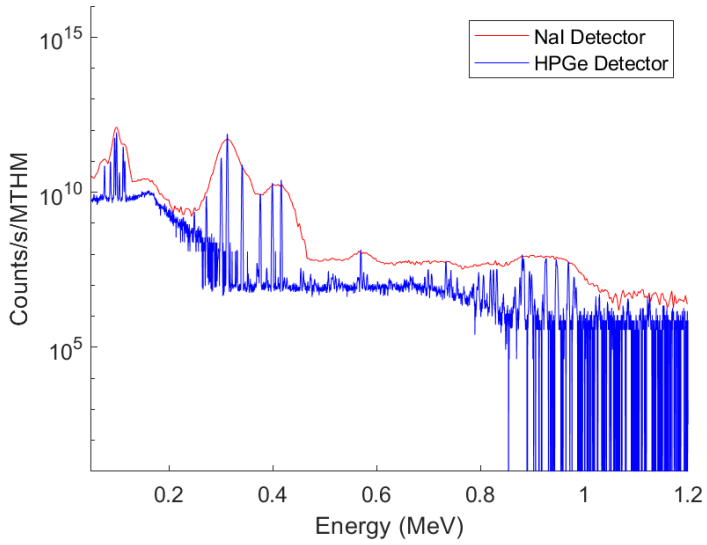

Figure D-3: Gamma spectrum for PWR at 1 day.

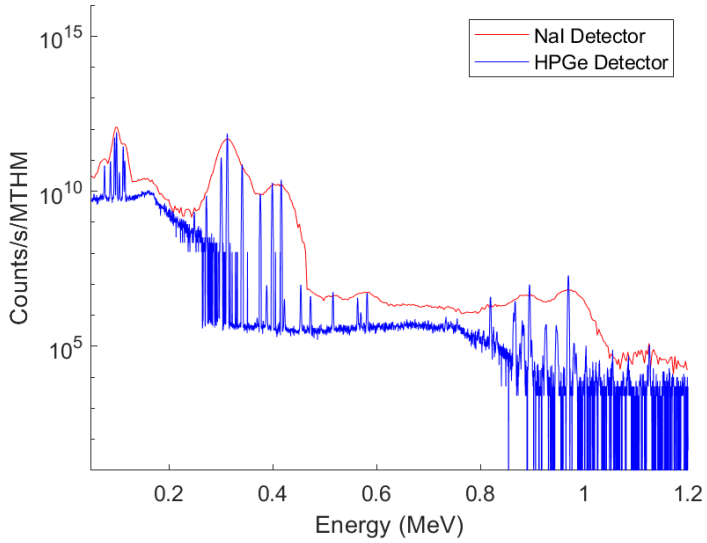

Figure D-4: Gamma spectrum for PWR at 3 days.

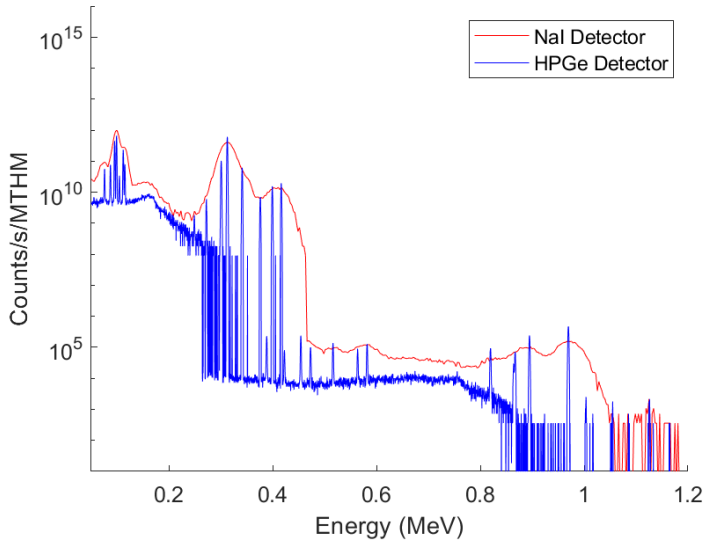

Figure D-5: Gamma spectrum for PWR at 10 days.

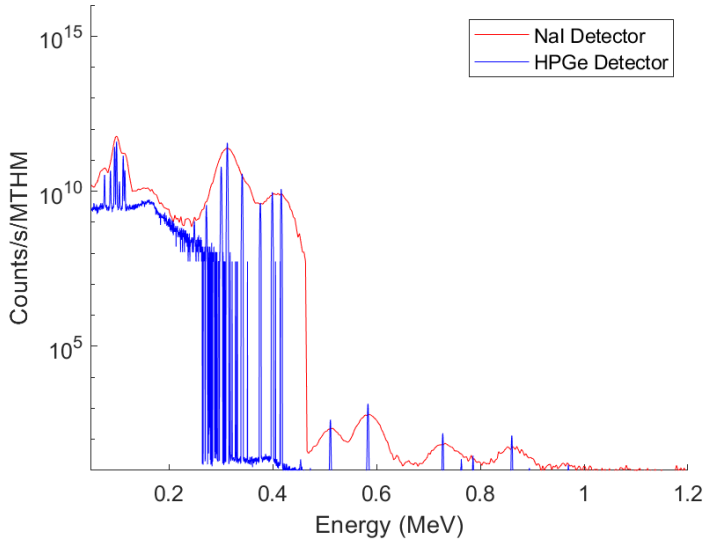

Figure D-6: Gamma spectrum for PWR at 30 days.

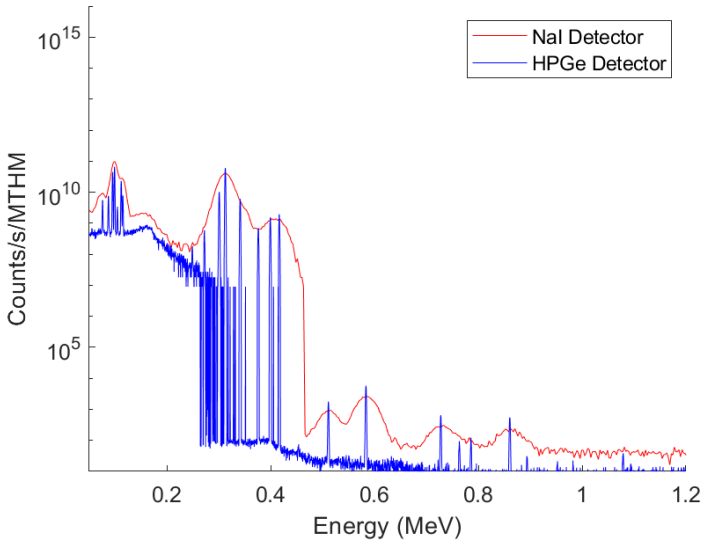

Figure D-7: Gamma spectrum for PWR at 100 days.

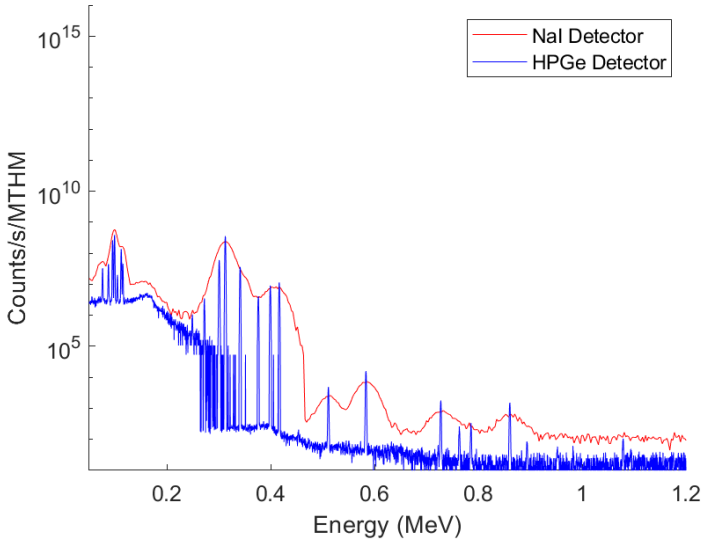

Figure D-8: Gamma spectrum for PWR at 300 days.

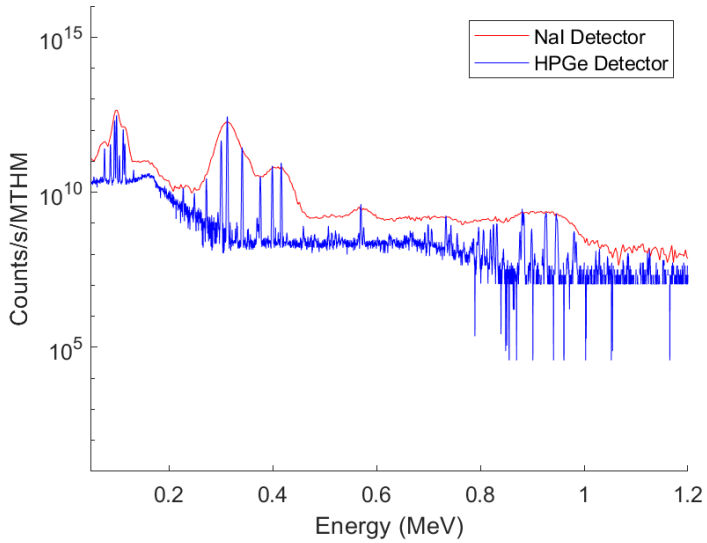

Figure D-9: Gamma spectrum for CANDU (0.711% enriched uranium) at 0 days.

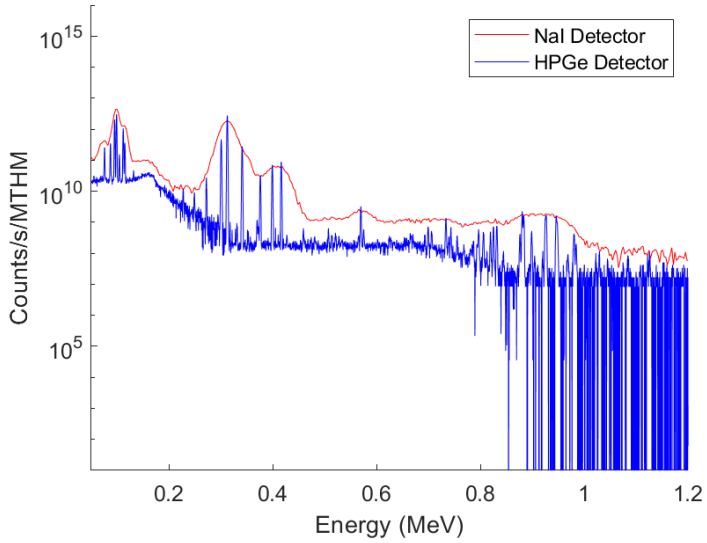

Figure D-10: Gamma spectrum for CANDU (0.711% enriched uranium) at 0.1 days.

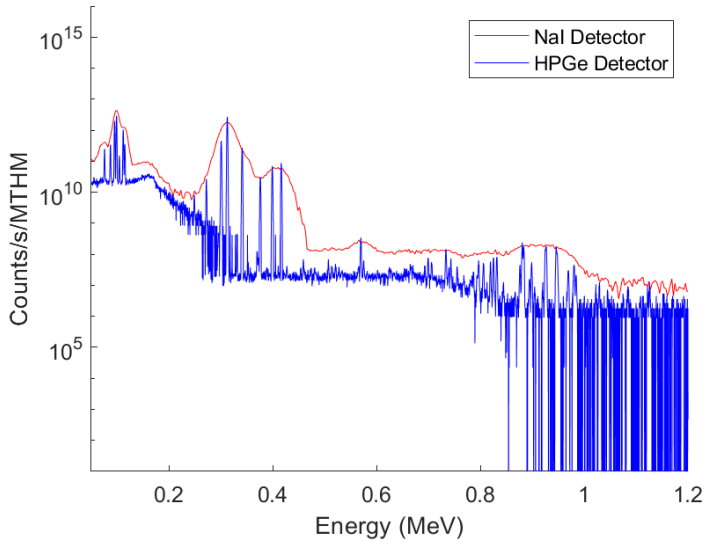

Figure D-11: Gamma spectrum for CANDU (0.711% enriched uranium) at 1 day.

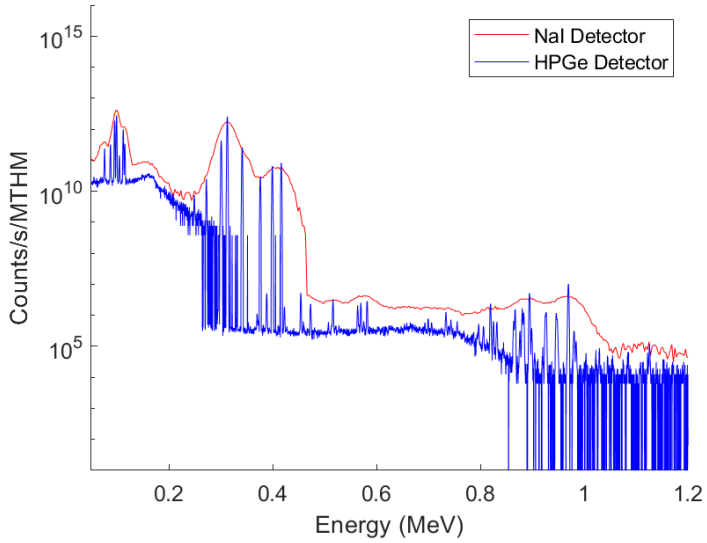

Figure D-12: Gamma spectrum for CANDU (0.711% enriched uranium) at 3 days.

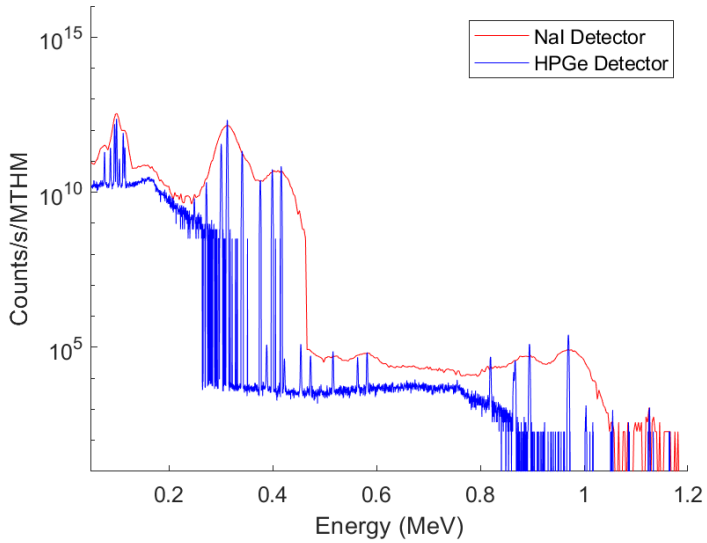

Figure D-13: Gamma spectrum for CANDU (0.711% enriched uranium) at 10 days.

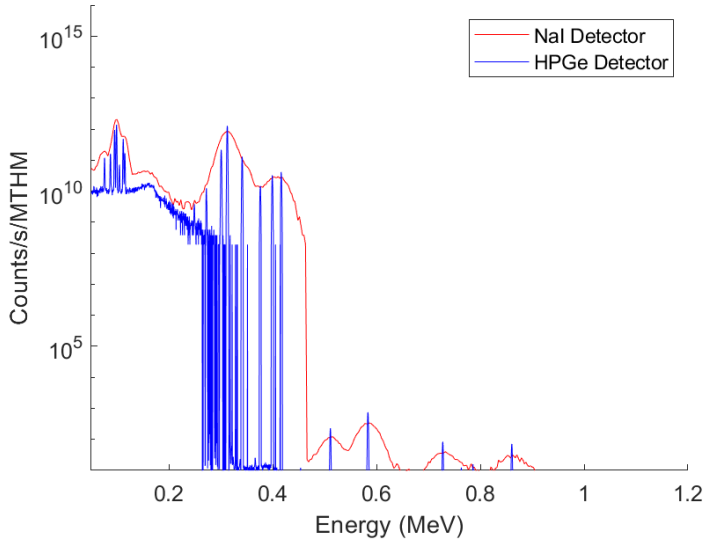

Figure D-14: Gamma spectrum for CANDU (0.711% enriched uranium) at 30 days.

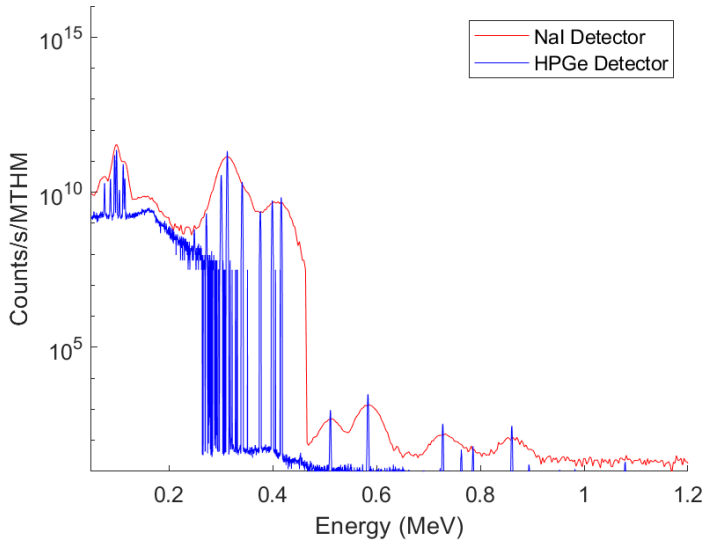

Figure D-15: Gamma spectrum for CANDU (0.711% enriched uranium) at 100 days.

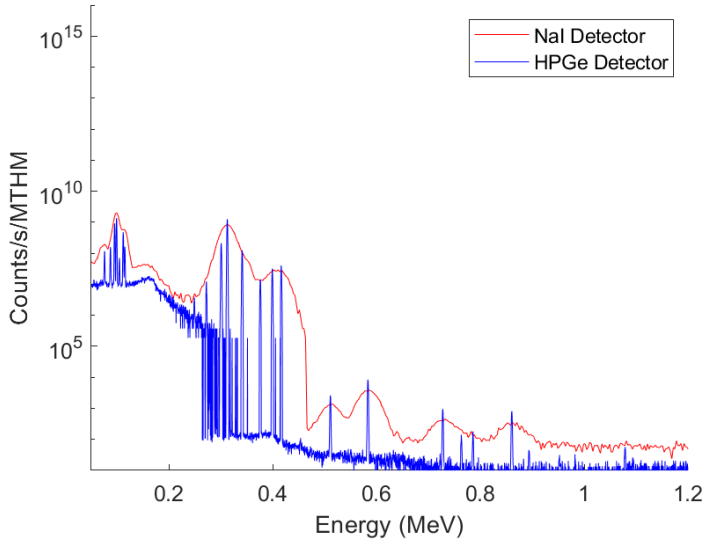

Figure D-16: Gamma spectrum for CANDU (0.711% enriched uranium) at 300 days.

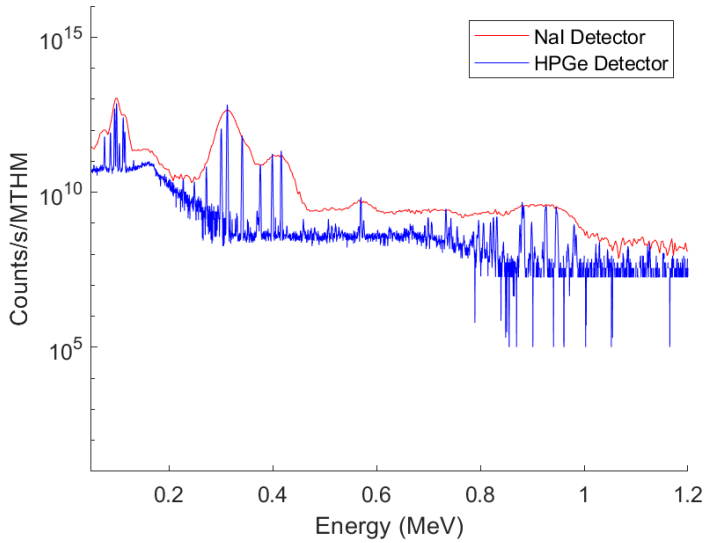

Figure D-17: Gamma spectrum for CANDU (19.7% enriched uranium) at 0 days.

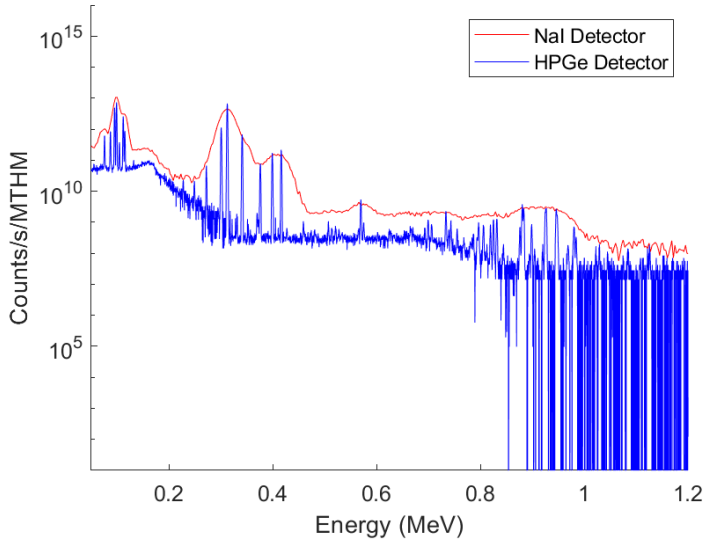

Figure D-18: Gamma spectrum for CANDU (19.7% enriched uranium) at 0.1 days.

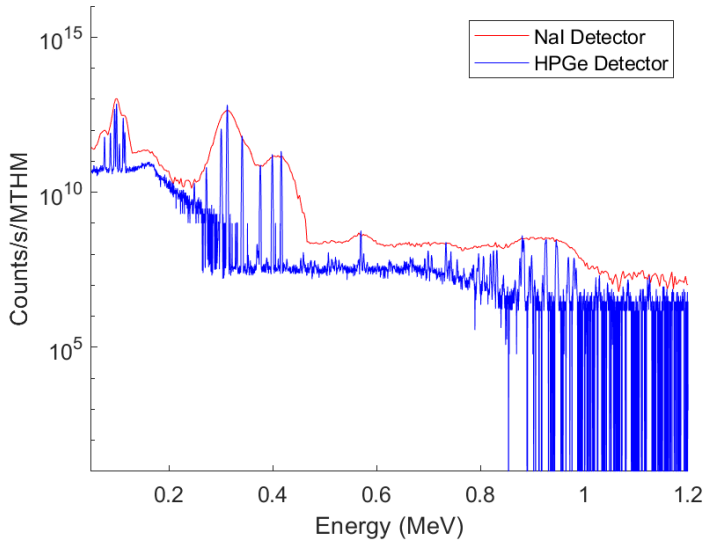

Figure D-19: Gamma spectrum for CANDU (19.7% enriched uranium) at 1 day.

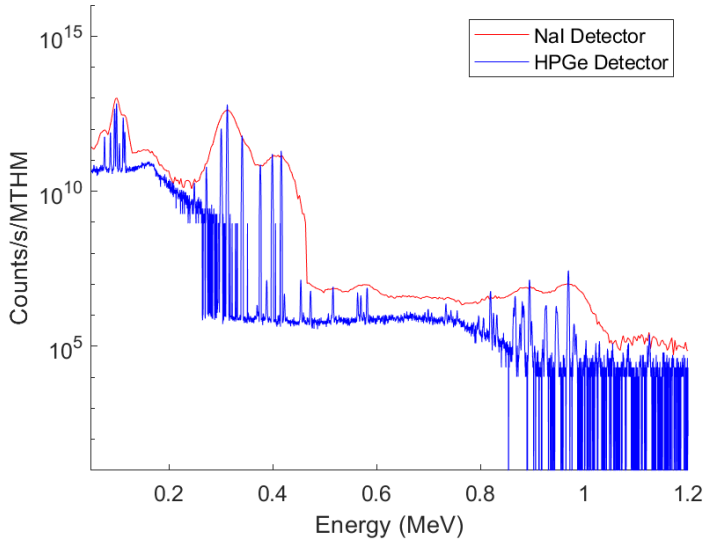

Figure D-20: Gamma spectrum for CANDU (19.7% enriched uranium) at 3 days.

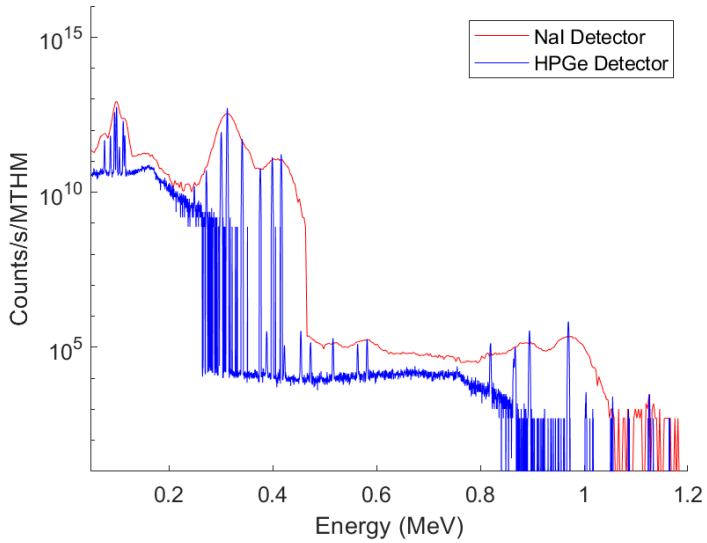

Figure D-21: Gamma spectrum for CANDU (19.7% enriched uranium) at 10 days.

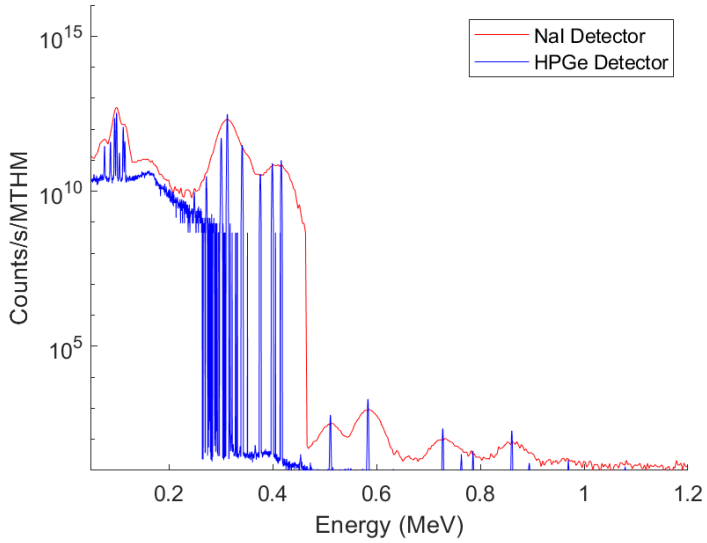

Figure D-22: Gamma spectrum for CANDU (19.7% enriched uranium) at 30 days.

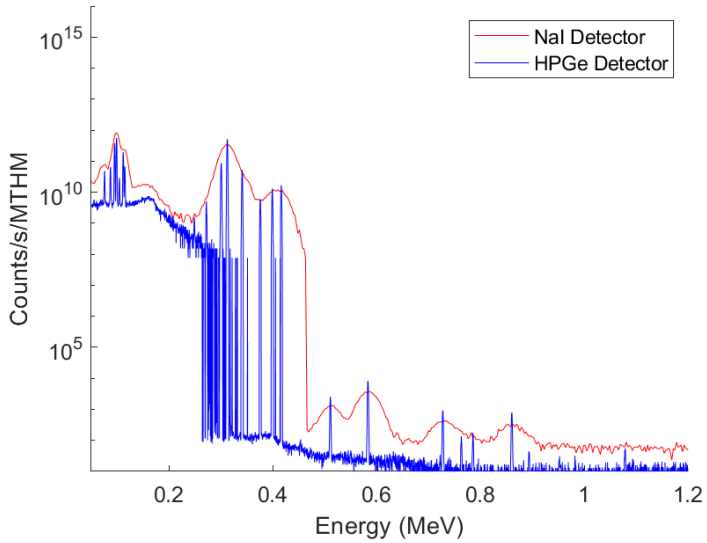

Figure D-23: Gamma spectrum for CANDU (19.7% enriched uranium) at 100 days.

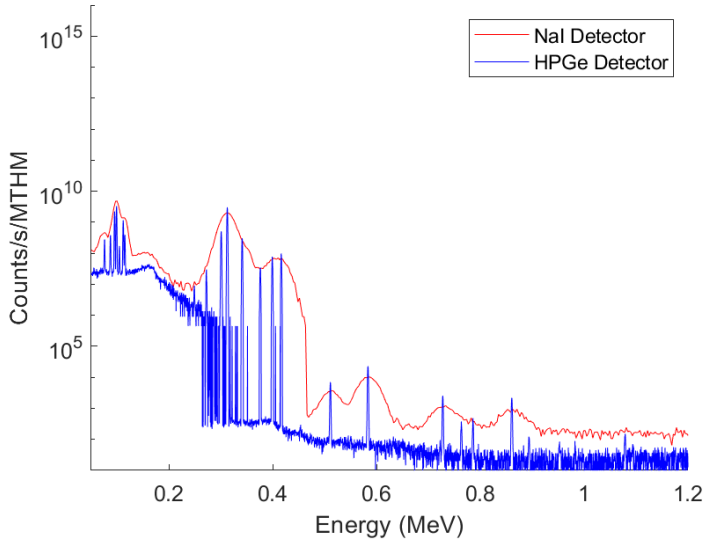

Figure D-24: Gamma spectrum for CANDU (19.7% enriched uranium) at 300 days.

Appendix E: GAMMA SPECTRA FOR SEPARATED PROTACTINIUM MIXTURE FOR SCALE TRITON SIMULATIONS

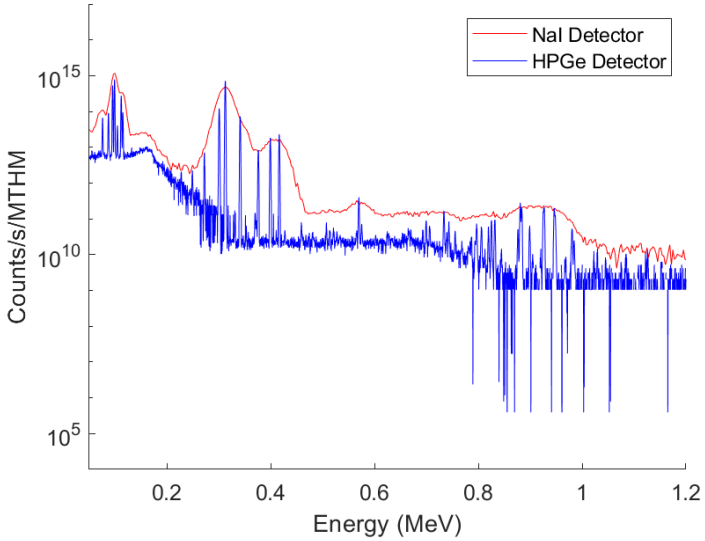

Figure E-1: Gamma spectrum for MSR at 2 days.

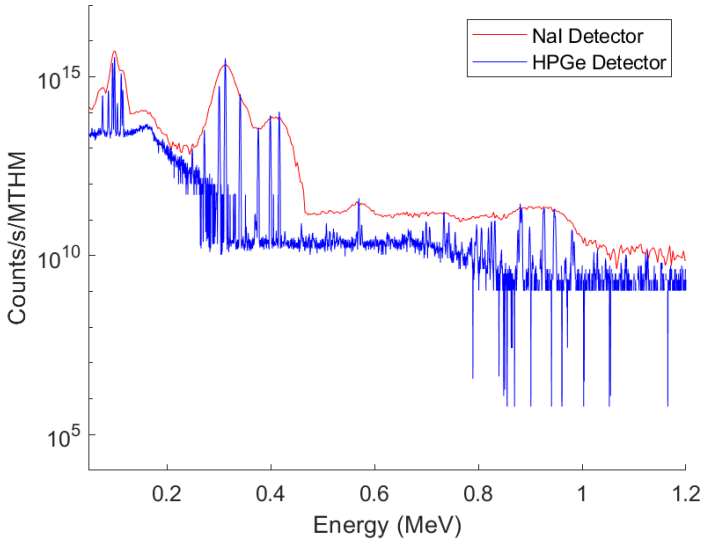

Figure E-2: Gamma spectrum for MSR at 10 days.

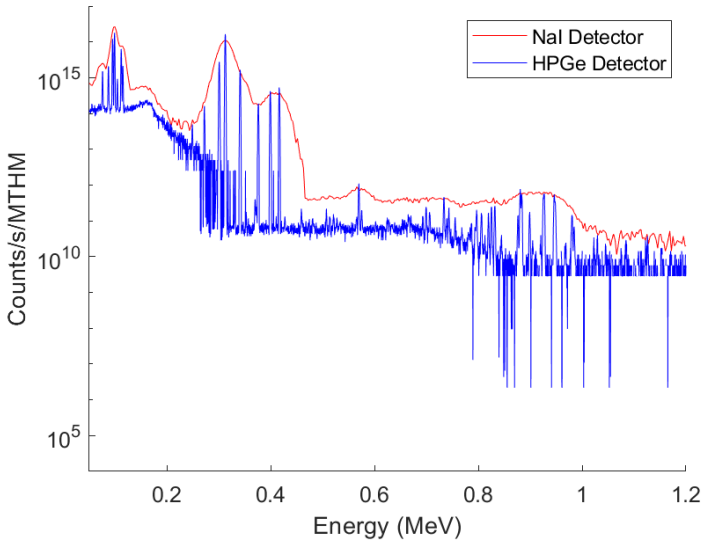

Figure E-3: Gamma spectrum for MSR at 30 days.

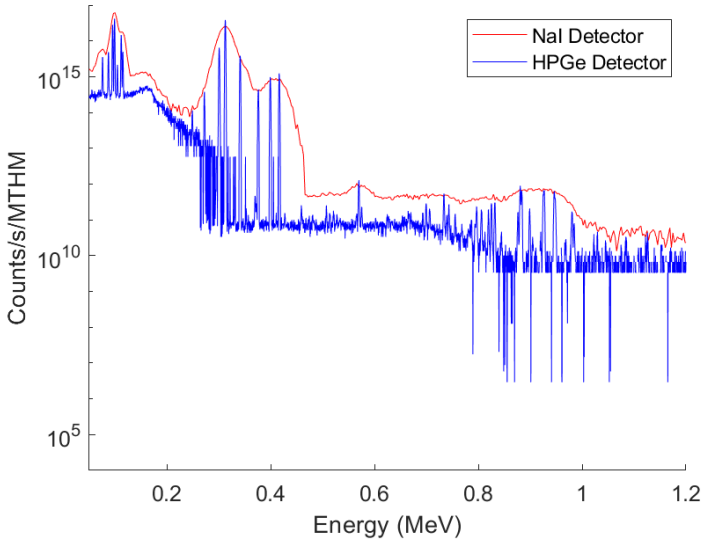

Figure E-4: Gamma spectrum for MSR at 100 days.

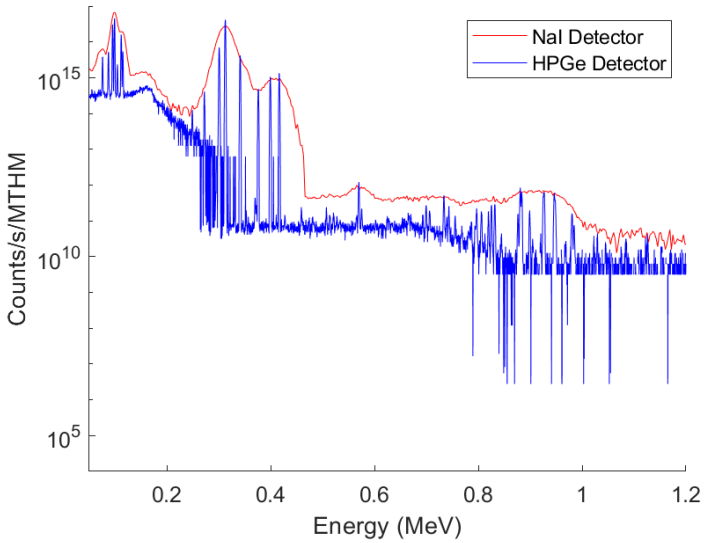

Figure E-5: Gamma spectrum for MSR at 300 days.

Strategic Security Sciences Division
Argonne National Laboratory
9700 South Cass Avenue
Lemont, IL 60439

www.anl.gov

Argonne National Laboratory is a U.S. Department of Energy laboratory managed by UChicago Argonne, LLC